fuels

MDPI

Article

Numerical Investigation of Performance, Combustion, and Emission Characteristics of Various Microalgae Biodiesel on CI Engine

Madeeha Rehman, Sujeet Kesharvani and Gaurav Dwivedi *

Energy Centre, Maulana Azad National Institute of Technology, Bhopal 462003, India
* Correspondence: gdiitr2005@gmail.com

Abstract: Biodiesel is being considered a possible alternative fuel due to its similarity with diesel and environmental benefits. This current work involves a numerical investigation of CI engine characteristics operating on D100 (diesel) and Dunaliella tertiolecta (DMB20), Scenedesmus obliquus (SOMB20), Scenedesmus dimorphu (SDMB20), and Chlorella protothecoides (CMB20) microalgae biodiesel blend. A diesel engine of 3.7 kW was used with variable compression ratios (CRs) (15.5, 16.5, 17.5, and 18.5) and constant speed (1500 rpm). Comparative analysis was performed for engine characteristics, including emission, combustion, and performance. Cylinder pressure, heat release rate, brake thermal efficiency, specific fuel consumption, particulate matter, oxide of nitrogen, carbon dioxide, etc., were evaluated using the blended fuel. The results show that the maximum cylinder pressure falls, SFC increases, and EGT and BTE were reduced for all blends at full load. In terms of emission characteristics, PM and smoke were lowered when compared to diesel, but a slight increment in NOx and CO_2 was observed. Among all the blends, SOMB20 shows the most decrement in PM and smoke emissions by 14.16% and 11.6%, respectively, at CR 16.5. CMB20 shows a maximum increment in SFC by 3.22% at CR 17.5. A minimum reduction in CP and HRR was shown by DMB20 irrespective of CRs.

Keywords: compression ignition engine; microalgae biodiesel; numerical simulation; performance; emission

Citation: Rehman, M.; Kesharvani, S.; Dwivedi, G. Numerical Investigation of Performance, Combustion, and Emission Characteristics of Various Microalgae Biodiesel on CI Engine. *Fuels* **2023**, *4*, 132–155. https://doi.org/10.3390/fuels4020009

Academic Editors: Toufik Boushaki and Elna Heimdal Nilsson

Received: 25 October 2022
Revised: 16 February 2023
Accepted: 24 March 2023
Published: 29 March 2023

1. Introduction

As the world's population grows, technology advances and people's living standards rise, so does energy consumption. In the not-too-distant future, uncontrolled fossil fuel exploitation could lead to the depletion of petroleum supplies [1]. The massive increase in fossil fuel consumption is due to rapid industrialization and an increment in the number of vehicles [2]. Industrial, transportation, and agriculture sectors utilize the majority of the energy generated by various sources, such as nuclear power, solar, wind, wood, petroleum, and coal [3,4]. Figure 1 depicts the the shares of world oil final consumption from 1973 to 2020 [5–7].

Among biofuels, biodiesel is a promising renewable substitute directly utilized in compression ignition (CI) engines without basic modifications [8]. Biodiesel is carbon neutral; oxygenated fuel contains about 10 wt.% of oxygen due to ester compounds which improve burning efficiency and have low sulfur content. Due to these properties, the emission of PM, CO, HC, SO2, and other gaseous pollutants are lowered compared to diesel [9,10]. The application of biodiesel blends can also ease dependency on the world's oil supply [11]. Diesel engine performance parameters also improve when biodiesel is used in diesel engines [12]. It includes several benefits compared to diesel fuel, including renewability, increased flash point, better cetane number, lower exhaust emissions, and so on [13,14]. Biodiesel is derived from different generations of oil feedstocks. Generally categorized into first, second, third, and fourth generations based on the sources from

which it is derived [15]. Figure 2 shows the different generations of feedstocks, their benefits, and their limitations.

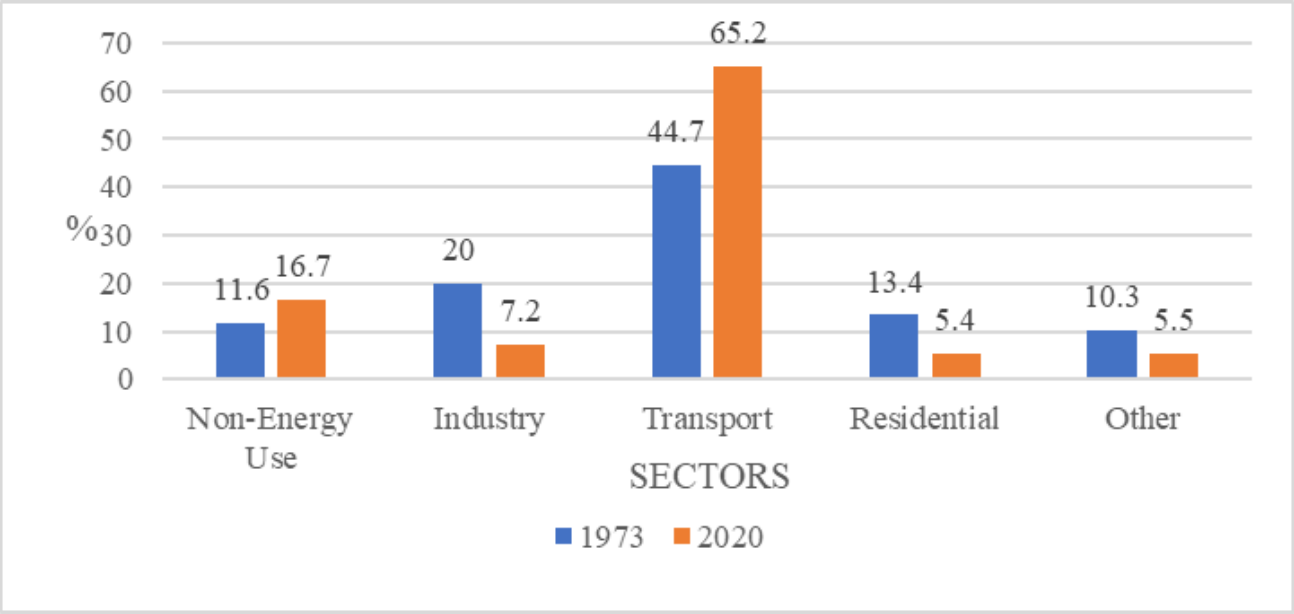

Figure 1. The shares of world oil final consumption from 1973 to 2020 [5–7]

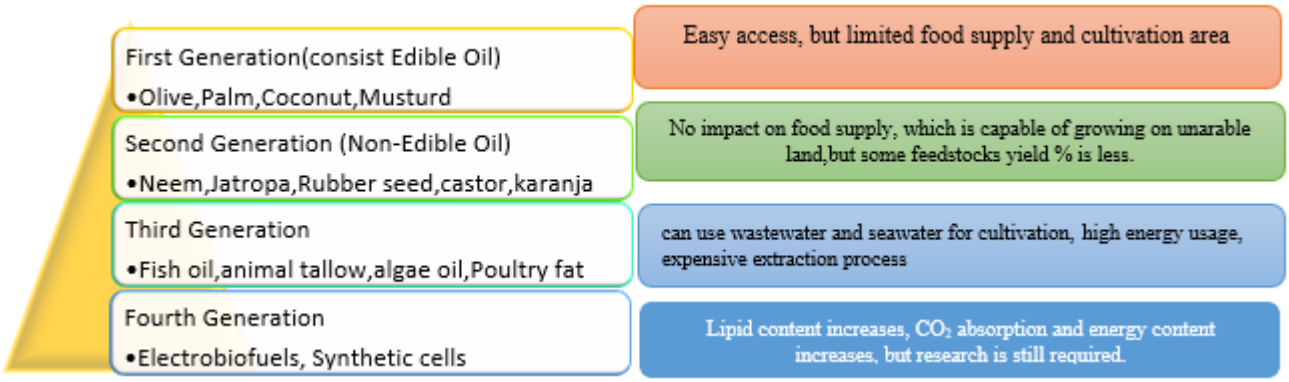

Figure 2. Different generation biodiesel production feedstocks; benefits and limitations [16].

In these four generations, many researchers have worked with the main focus on resources. Among these, third-generation microalgae are found to be auspicious renewable energy feedstocks, as they can directly be converted into biodiesel [17]. Microalgae have several advantages that make biodiesel produced from them a more suitable substitute for conventional fuel. It has a yield of 58,700 L of oil per hectare, which is converted into 121,105 L of biodiesel [18]. Increased productivity could also result in much higher biomass outputs a day per unit cultivated area [19,20]. The major advantage is that it can be grown on arid land and in wastewater, which offers a way to remove phosphorus, nitrogen, and metal from wastewater and even requires fewer nutrients [21]. However, the cost of production is high, as there are several energy-intensive steps for oil extraction [22,23]. Sulfur is absent, and there are fewer pollutant emissions, such as particulate matter, CO, hydrocarbons, and Sox. NOx emissions seem to be higher in some engines due to elevated temperatures in a combustion chamber. Still, some literature shows algae biofuel blends produced less NOx than diesel fuel [24,25]. Microalgae emerged as the only renewable biodiesel source able to meet the international demand for transportation fuel, with the likelihood of replacing the existing use of fossil fuels and shifting to the use of biodiesel [26].

D. tertiolecta, because of its fast growth rate and potential to develop in brackish environments, is a strong choice for biofuel production. Moreover, the ash content varied from 0.2 to 0.5% [27]. The high C18:3 concentration of D. tertiolecta biofuel may result in poor oxidative stability [28]. However, the lipid profile, which is primarily composed of unsaturated and saturated FA, is similar to those produced from other oils used in biodiesel production [29]. As emission analysis conducted on the D. tertiolecta blend shows, the use of B20 and B10 biodiesel produced emissions against diesel fuel an average decrease in CO, HC, and NOx emissions for B10 and B20 is 9.21%, 7.32%, and 2.89%, and 23.54%, 18.28%, and 6.97%, respectively. As for engine performance, output power for the B20 blend was lowered by 2.64%, and BSFC shows a rise of 3.64% when compared to diesel. Overall, the results show that D. tertiolecta is capable of clean fuel [30].

For biodiesel production, S. obliquus had the maximum lipid content, with MUFAs and SFAs predominating [31]. S. obliquus had high oleic acid (17.4%) and palmitic acid (23.4%) content, which complied with European biodiesel legislation. S. obliquus is a high-performance biofuel that is utilized in a 20% blend in diesel engines [32]. The iodine value, ash content, and water content were within biodiesel standards limits, i.e., international and Indian standards. The saponification amount was found between 239.4 and 244.8 mg KOH/g; however, its cetane index varied between 51.3 and 54.0 [33]. Thus, this study recommends S. obliquus as a viable feedstock for biodiesel generation.

Scenedesmus dimorphus was observed to be a better alternative for biodiesel feedstock due to its high proportion of Saturated, Monounsaturated, and Polyunsaturated fatty acids [31]. Scenedesmus dimorphus algae is a better and safer alternative to oil-based fuels, having about 50% oil by weight [34]. For the biodiesel–diesel blends, the engine characteristics show a significant rise in SFC with low BP. Except for NOx, all diesel blends showed a decrease in GHG emissions [35].

When diesel fuel was combined with 20% microalgae biodiesel made from Chlorella protothecoides, the tractor engine's (25.8 kW) performance and emissions characteristics were assessed. B20 had a cetane number of 49.6 and an HHV of 44.8 MJ/kg, both of which were comparable to standard diesel fuel, but increased viscosity and density values were observed. The results show that using the microalgae biodiesel blend has no discernible impact on engine performance, but it significantly reduces brake power (0.77 kW) when used to power a tractor [36].

In India, to perform experimental investigation, samples can be collected from various locations: Dunaliella tertiolecta at the Western India coastline, and Sambhar Salt Lake in Rajasthan [37,38]; Scenedesmus obliquus at Guwahati, Assam (26°1101500 N 91°450400 E) [39]; Scenedesmus dimorphu at Chandrapur area, North-East, Assam, India, and Aulakhpur village, Muktsar, India [40,41]; and Chlorella protothecoides at Kovalam solar salt Kanyakumari, India [42]. Previous researchers have performed studies using samples from these areas.

Several pollutants can be lowered by employing biodiesel, except for NOx, which is generally reported due to higher combustion temperatures [15,24]. Instead, blends or straight biodiesel emulsions can be used, and they show a promising decrement in CO_2 and NOx emissions [43]. However, a few findings for testing the engine contain contradictions also omit crucial information. So, a further detailed investigation is needed.

This research intends to examine the CI engine's characteristics using Dunaliella tertiolecta, Scenedesmus obliquus, Scenedesmus dimorphu, and Chlorella protothecoides microalgae. There is limited literature available on the comparative evaluation of different microalgae biodiesels and diesel and on the performance of diesel engines with varying CR (compression ratio). Therefore, this study provides a brief microalgae biodiesel comparison using a numerical technique. In this paper, firstly, for a Diesel-RK model, experimental validations with various engine characteristics employing diesel fuel were performed at constant CR 17.5 from previous research. Secondly, the performance, combustion, and emission parameters for Dunaliella tertiolecta, Scenedesmus obliquus, Scenedesmus dimorphu, and Chlorella protothecoides microalgae 20% blend biodiesel were studied

using a single-cylinder diesel engine (3.7 kW power), constant speed (1500 rpm), variable compression ratio (15.5,16.5,17.5,18.5), and fixed injection timing of 23.5° before TDC.

2. Materials and Methods

2.1. Test Fuel Properties

Microalgae biodiesel has several environmental and land use benefits not only confined to higher photosynthetic efficiencies [44]. Microalgal oil has unique features such as greater unsaturation levels. The amount of research that has looked into the possibility of using algal biodiesel in engines is inadequate to provide a complete picture of how this fuel will perform. As a result, the evaluation of their application in internal combustion engines is essential [45]. The Dunaliella tertiolecta, Scenedesmus obliquus, Scenedesmus dimorphu, and Chlorella protothecoides microalgae biodiesels have been chosen for analysis in this research. Table 1 enlist the Physicochemical properties of various biodiesel fuels [30,32,35,46–48].

Table 1. Physicochemical properties of biodiesel fuels [30,32,35,46–48].

Fuel Properties	EN Standard	IS Standard	Diesel	*Dunaliella tertiolecta*	*Scenedesmus obliquus*	*Scenedesmus dimorphu*	*Chlorella protothecoides*
Density at 15 (kg/m^3)	860–900	870–900	850	890	863	862	881
Kinematic viscosity ($m^2\ s^{-1}$ at 40 °C)	3.5–5	2.5–6.0	2.6	4.2	4.09	4.14	4.491
Cetane no	≥51	≥51	49–55	54	63.2	37.1	57.3
Higher Heating Value (MJ/kg)			42.2	40.2	42.11	42.13	37.56
Ash content (%)	<0.02	<0.02	0.01	-	-	-	0.01
Flashpoint (°C)	101	120	73	-	-	-	141
Pour Point (°C)	-			-	−16	−16	
Specific gravity (°C)	-	-		-	0.84	0.82	-
Acid Value (mg KOH/g)	<0.5	≤0.8	0.4	-	0.38	0.33	0.21

In comparison to the other blends tested, the B20 blend has shown a precise estimation with diesel properties, which results in higher BTE and lower CO and HC, along with lower smoke and PM emissions [49]. As a result, Diesel-RK's investigation of all microalgae biodiesel employed a B20 blend for the study of various parameters. The 20% biodiesel blend was created based on volume to analyze the engine according to ASTM standards. The prepared blends were DMB20, SOMB20, SDMB20, and CMB20. (The number signifies the percentage of microalgae biodiesel: 20% and 80% diesel.)

Figure 3 shows the blends of volumetric composition (%) used in this study. The fuel characteristics were evaluated for the biodiesel blends DMB20, SOMB20, SDMB20, and CMB20 that are used in the software listed in Table 2.

Table 2 describes the properties of microalgae biodiesel fuel and its blend, which were used during the analysis.

2.2. Experimental Setup

This numerical investigation through Diesel-RK software version 4.3.0.189 was conducted using a model consisting of a stationary natural aspiration, single-cylinder, water-cooled diesel engine with direct injection operating at a constant engine speed of 1500 rpm and producing 3.7 kW of rated power. The analysis was conducted under various load situations (25%, 50%, 75%, and 100%), and compression ratios (15.5, 16.5, 17.5, and 18.5).

The detailed test engine specifications used during analysis are listed in Table 3. These specifications were ensured using a test engine setup done in software. Figure 4 shows the test engine setup systematic diagram. The test engine was comprised of the following components: an eddy current dynamometer, an exhaust calorimeter, a control system, a load cell, a sensor, a rotameter, a flue gas analyzer, and a control system. Engine torque was

by measurement of eddy current dynamometer of speed range of 0–1500 rpm, and torque range of 0–2.4 k.gm was coupled with an engine.

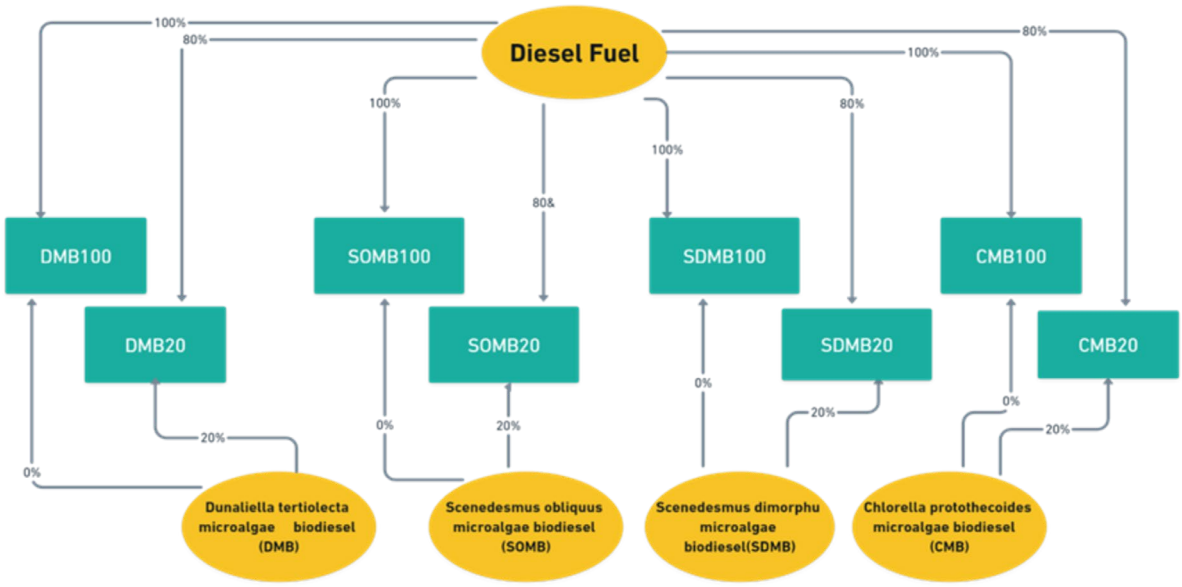

Figure 3. Blends volumetric composition of test fuel (%).

Table 2. Physicochemical properties of obtained biodiesel blends.

Properties	Diesel	DMB_{20}	$SOMB_{20}$	$SDMB_{20}$	CMB_{20}
C (% *w*/*w*)	0.87	0.843	0.82899	0.844	0.8472
H (% *w*/*w*)	12.6	0.119	0.12189	0.123	0.124
O (% *w*/*w*)	0.4	0.116	0.04912	0.321	0.0278
Cetane Number	52	49.317	51.764	46.234	50.137
LHV (MJ/kg)	42.5	42.06	42.422	42.426	41.606
Dynamic Viscosity coefficient (Pas @ 40 °C)	0.003	0.00353	0.00341	0.00345	0.0038
Density (kg/m^3 @ 15 °C)	830	843.68	836.80	836.59	840.69

Table 3. Engine specifications of a test engine.

Engine Parameter	Specification
Model	Kirloskar Model TV 1
Type	Direct-injection diesel engine
Rated power(kW)	3.7
Stroke(mm)	110
Bore(mm)	80
Type of cooling	water
No of cylinder	Single
CR	15.5:1,16.5:1,17.5:1,18.5:1
Speed (rpm)	1500
Dynamometer type	Eddy current
Fuel injection type	Higher-pressure common rail
Injection timing	23.5 (deg. before TDC)
Exhaust valve closing	4.5 (deg. before TDC)
Exhaust valve opening	35.5 (deg. before BDC)
Inlet valve closing	35.5 (deg. after BDC)
Inlet valve opening	4.5 (deg. before TDC)
Fuel pressure	500–800 bar
Number of the nozzle and hole diameter (mm)	3.0 and 0.25
Piston type	120 deg.

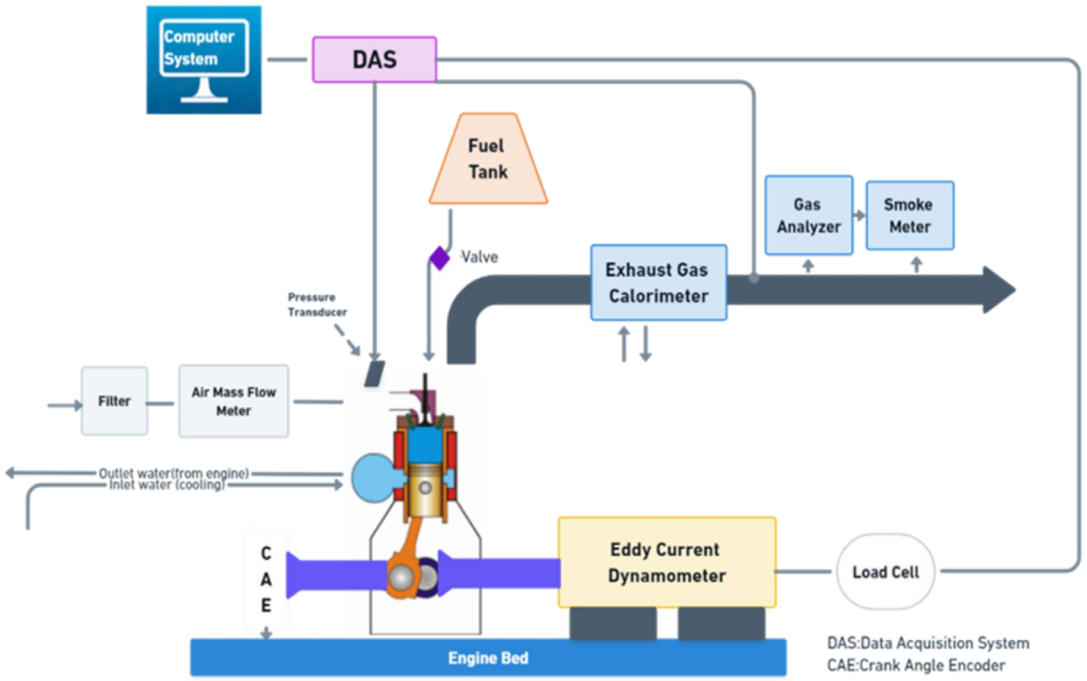

Figure 4. Test engine setup.

2.3. Uncertainty Analysis

Experimental work requires uncertainty and error analysis to ensure the calculated parameter is accurate. This work has covered a variety of errors (calibration, accuracy of equipment, environmental conditions, and other factors). In this study, load, speed, pressure, smoke meter, and crank position indicators were all used as instruments with specifications by the researchers. For the measurement of flue gases, a 350-Testo was used.

The uncertainties connected with the detectors used in this study are presented in Table 4. The standard deviation equation was used to get the overall proportion of uncertainty, which was previously published in the literature [50–52].

$$\begin{aligned}\text{Uncertainity} = \sqrt{(\text{Speed Sensor})^2 + (\text{Local Cell Sensor})^2 + (\text{Digital stop watch})^2 + } \\ (\text{Eddy current dyanometer})^2 + (\text{Crank angle encoder})^2 + (\text{Smoke meter})^2 + \\ (\text{Speed Sensor})^2 + (CO_2)^2 + (NO_X)^2 + (CO)^2 + (HC)^2\end{aligned} \quad (1)$$

Following the preceding Equation (1), the composite uncertainty was calculated to be ±1.52%, which was under the permissible limit [53,54].

Table 4. Experimental test engine's instrumentation and uncertainties.

Instruments		Range	Accuracy	Uncertainties
Smoke meter		BSU 0–100	±1%	±1.0%
Crank angle encoder		±0.5 CA	± 0.2 °CA	±0.2%
Load indicator		0–100 kg	±1 kg	±0.2%
Eddy current dynamometer		-	-	±0.15%
Testo 350 gas analyzer	NOx	0–3000 ppm	±5% reading	±0.5%
	HC	0–40,000 ppm	±10% of reading	±0.1%
	CO	0–10,000 ppm	±10 ppm < 200 ppm	±0.3%
	CO_2	0–50 vol%	±0.3% < 25 vol%	±1%
Digital stopwatch		-	±0.2 s	±0.2%
Speed sensor		-	-	±0.1%
Load indicator		-	-	±0.2%

2.4. Numerical Tool

2.4.1. Diesel-RK Model

A simulation tool for numerically analyzing engine performance is the Diesel-RK model. It is based upon Thermodynamics' First Law and is required for advanced diesel combustion simulation and emission formation prediction. With the help of this software, temperature, pressure, and additional important parameters are calculated in accordance with the crank angle or time. To take into consideration the friction and heat emission of the engine, semi-empirical correlations generated from experimental data are used. The engine's combustion process is simulated using a multi-zone model. It calculates NO_X emissions using the Zeldovich mechanism [50,55].

2.4.2. Simulation Models

The Diesel-RK engine models are chosen for their correctness, computation speed, and generality.

Table 5 contains a list of the models that were used in the simulation and their descriptions. A multizone model is used to calculate combustion in engines. The Wiebe technique calculates heat release rate. In this software system, the Zeldovich mechanism is employed to compute nitric oxide. A heat transfer equation determines the surface temperatures. The Woschni formula determines the gas-wall heat transfer coefficient.

Table 5. Simulation models in Diesel-RK.

Sr. No.	Parameter	Models
1	Combustion	Multi-Zone Model
2	Ignition Delay	Tolstov's Mechanism
3	Smoke	Bosch and Hartridge mechanism
4	Rate of heat release	Wiebe method
5	NO	Thermal Zeldovich mechanism
6	PM	Alkidas formula
7	Soot	Razleytsev Mechanism
8	Heat transfer	Woshchni's formula

2.4.3. Governing Equations

Governing equations that were used for the simulation models for the analysis of different parameters in Diesel-RK and previous research are shown in Table 6 [56–60].

2.4.4. Simulation Inputs

Several characteristics (including CP, HRR, BTE, SF, EGT, specific carbon dioxide and nitric oxide emissions, specific particulate matter, and smoke level (BSN)) are calculated, as stated in Table 7, at CR (15.5, 16.5, 17.5, and 18.5) at a constant speed and variable load (25%, 50%, 75%, 100%). All these variations are tested for Diesel (D100) and microalgae biodiesel blends (DMB20, SOMB20, CMB20, and SDMB20). The results were compared and analyzed based on variations in CR, load, and use of diesel and microalgae biodiesel blends as fuel. Table 7 depicts the matrix of simulation work performed in this current research.

2.5. Diesel-RK Model Validation

The Diesel-RK simulation results are validated against the results of experiments taken by Upendra Rajak and Prerana Nashine (2019) [61] on a single-cylinder diesel engine for cylinder pressure, BTE, and EGT. The comparison of parameters was performed on 100% engine load and using test engine specifications, as shown in Table 3.

Table 6. Governing equations in Diesel-RK.

System	Equation	Abbreviation
Conservation of mass	$\frac{dw}{dt} = \sum_j w_j$	w_j = mass flow rate of jth species (kg/s)
Conversion of species	$Y_j = \frac{w_j}{w}$	w = total mass within cylinder (kg)
Species equations	$\frac{d(wY_i)}{dx} = \sum_j \dot{m}_j Y_i^j + \dot{S}_g$	S_g = net generation of ith species (kg/s)
ith species net generation	$Y_i = \sum_j (\frac{w_j}{w})(Y_i^j - Y_i^{cyl}) + \frac{\Omega_i W_{mw}}{\rho}$	Ω_i = rate of molar(mol/s) P = density (kg/m^3)
Energy balance	$\frac{d}{dt}(mu) = -p\frac{dv}{dt} + \frac{dQ_{ht}}{dt} + \sum_j \dot{m}_j h_j$	P= pressure (MPa)
Frictional means effective pressure	$FMEP = \alpha + \beta P_{\mathrm{m}} + \gamma V_p$	$\alpha = \beta = \gamma$ constants, P_{m} = Peak cylinder pressure(bar), V_p = mean piston velocity(m/s)
Brake-specific fuel consumption	$SFC = \frac{w_f}{brake\ power}$	w_f = mass flow rate(kg/s)
Heat release in ignition delay	$\tau = 3.8 \times 10^{-6}\ (1 - 1.6 \times 10^{-4} \times \mathrm{speed})\sqrt{\frac{\mathrm{T}}{\mathrm{P}}}\exp(\frac{\mathrm{E_a}}{8.312\mathrm{T}} - \frac{70}{\text{Fuel cetane number}})$	P = pressure, T = temperature $\mathrm{E_a}$ = Activation energy of fuel, τ = time (s)
Heat release in pre-mixed combustion	$\frac{dx}{d\tau} = \Phi_0 \times (A_0(m_f/v_i) \times (\sigma_{ud} - x_0) \times (0.1 \times \sigma_{ud} + x_0) + \Phi_1 \times (\frac{d\sigma_u}{d\tau})$	$\sigma_{ud} = \sigma_u$ = fuel fractions evaporated at ignition delay
Heat release during controlled combustion	$\frac{dx}{dt} = \Phi_0 \times \frac{d\sigma_u}{d\tau} + \Phi_2 \times (A_2(m_f/v_c) \times (\sigma_u - x) \times (\alpha - x))$	$\frac{dx}{d\tau}$= heat release rate (J/s) x = fraction of fuel burnt $\phi_0 = \phi_1 = \phi_2 = \phi_3 = \phi$ = crank angle
Heat release during late combustion	$\frac{dx}{dt} = \Phi_3 A_3 K_T (1 - x)(\xi_b \alpha - x)$	α = air-fuel ratio ξ_b = air efficiency
NOx formation modeling (Zeldovich mechanism)	$O_2 \leftrightarrow 2O$ $N_2 + O \leftrightarrow NO + N$ $N + O_2 \leftrightarrow NO + O$	O = Oxygen N = Nitrogen
Bosch Smoke Number	$[PM] = Z_{PM}\ 565 * (ln\frac{10}{10 - BN})^{1.206}$	PM = Particulate matter BN = Bosch Number
Hartridge smoke level	$\mathrm{H} = 100\{1 - 0.9545\ exp(-\ 2.4226[\mathrm{C}])\}$	

Table 7. Test matrix for simulation work.

Sr. No.	Input Parameter				Output
	Compression Ratio	Engine Speed (rpm)	Load (%)	Fuel Blend	
1	15.5 16.5 17.5 18.5	1500	25% 50% 75% 100%	D_{100} Blends (DMB_{20},$SOMB_{20}$ CMB_{20},$SDMB_{20}$)	CP HRR BTE SFC EGT Specific Carbon Dioxides Emission Nitric Oxide Emission Specific Particulate Matter Smoke Level (BSN)
2	15.5 16.5 17.5 18.5	1500	25% 50% 75% 100%	D_{100} Blends (DMB_{20},$SOMB_{20}$ CMB_{20},$SDMB_{20}$)	
3	15.5 16.5 17.5 18.5	1500	25% 50% 75% 100%	D_{100} Blends (DMB_{20},$SOMB_{20}$ CMB_{20},$SDMB_{20}$)	
4	15.5 16.5 17.5 18.5	1500	25% 50% 75% 100%	D_{100} Blends (DMB_{20},$SOMB_{20}$ CMB_{20},$SDMB_{20}$)	

Figure 5a,b, and c show the variation in values of simulated and experimental data of CP, BTE, and EGT temperature, respectively.

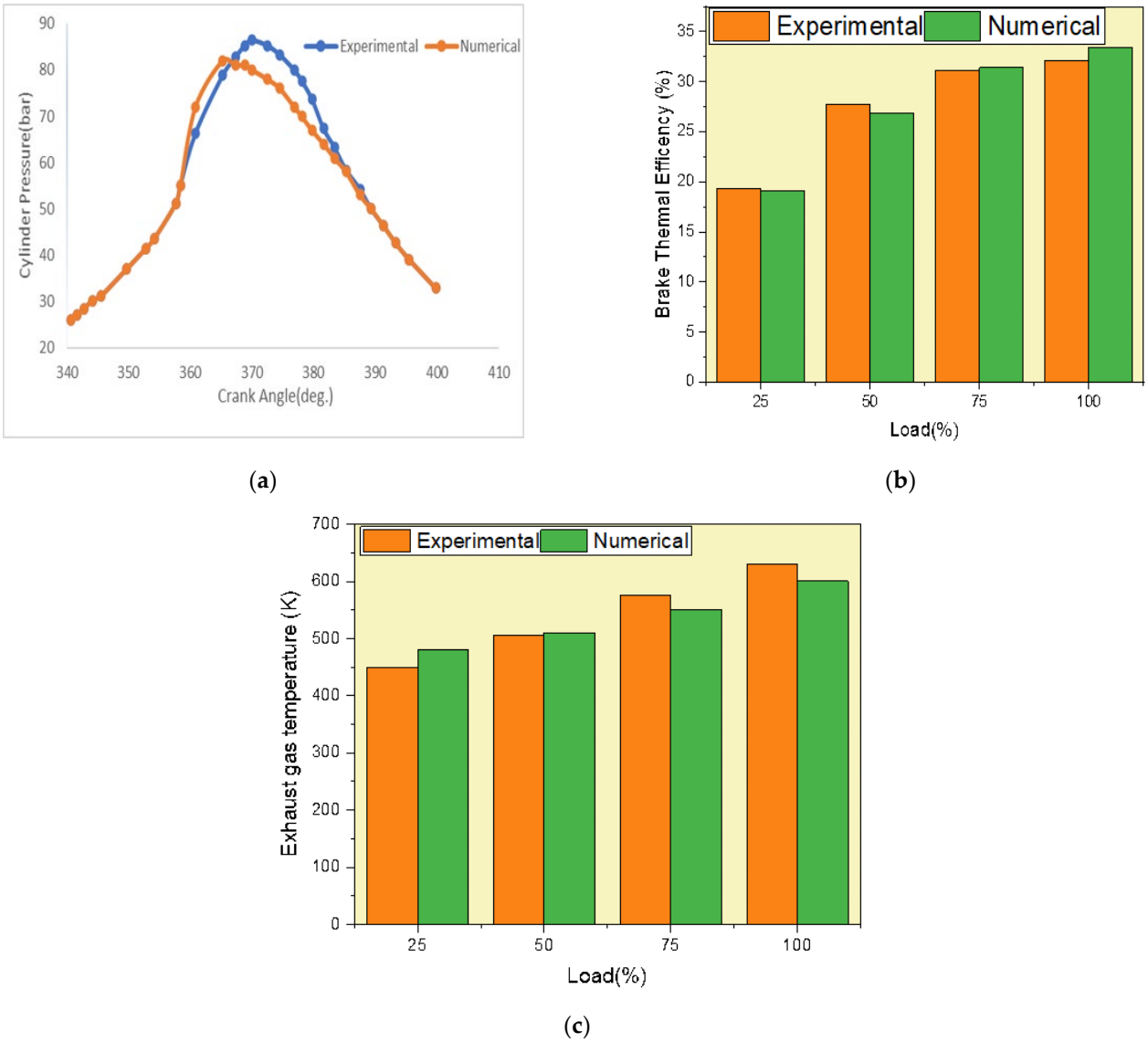

Figure 5. Comparison of experimental and simulated data for (**a**) CP, (**b**) BTE, and (**c**) EGT.

The largest error in CP was 4.61%, BTE was 3.7%, and EGT was 4.76% at full load, as shown between the investigated and simulation findings. As a result, the differences between experimental and numerical results are within acceptable tolerance limits. Table 8 shows remarkable agreement between computational and experimental results when the same conditions apply.

Table 8. Comparison of numerical and experimental results under 100% load condition.

Sr. No.	Parameter	Validation		
		Experimental Results	**Numerical Results**	**Error Deviation**
1	Maximum cylinder pressure (bar)	85.44	82.45	4.61%
2	Brake thermal efficiency (%)	32.2	33.4	3.7%
3	Exhaust gas temperature (K)	630	600.59	4.76%

3. Results

3.1. Combustion Parameters Analysis

3.1.1. Cylinder Pressure (CP)

CP is required to investigate the combustion chamber's behavior and to calculate the performance of the engine. The CP and rate of heat release (HRR) throughout combustion are dependent on the fuel combustion rate during the premixed combustion phase [62]. As CR increases, air–fuel mixture density also increases, which improves the mixing of burned and unburned charge and ultimately results in increased compression pressure [63]. When using alternative fuels, cylinder pressure is reduced due to greater viscosity, a lower atomization process, and a lower ignition delay during the combination of fuel and air, resulting in a rise in the rate of pressure buildup in the cylinder [64,65]. Therefore, compared to diesel, biodiesel's peak CP is lower [66].

Figure 6 shows the connection between crank angle and cylinder pressure for several tested microalgae biodiesel at full load conditions at varied CR (15.5, 16.5, 17.5, and 18.5). Figure 6 illustrates that the maximum cylinder pressure for D100, DMB20, SOMB20, CMB20, and SDMB20 obtained was 70.24 bar, 69.46 bar, 68.95 bar, 67.14 bar, and 67.2 bar, respectively, at 365 deg. crank angle for CR 15.5. From the numbers, it can be seen that peak CP rises as CR rises (15.5–18.5), but its values fall for biodiesel fuel when compared with diesel fuel. B.J. Bora et al. (2014) discovered similar variances in the result [67].

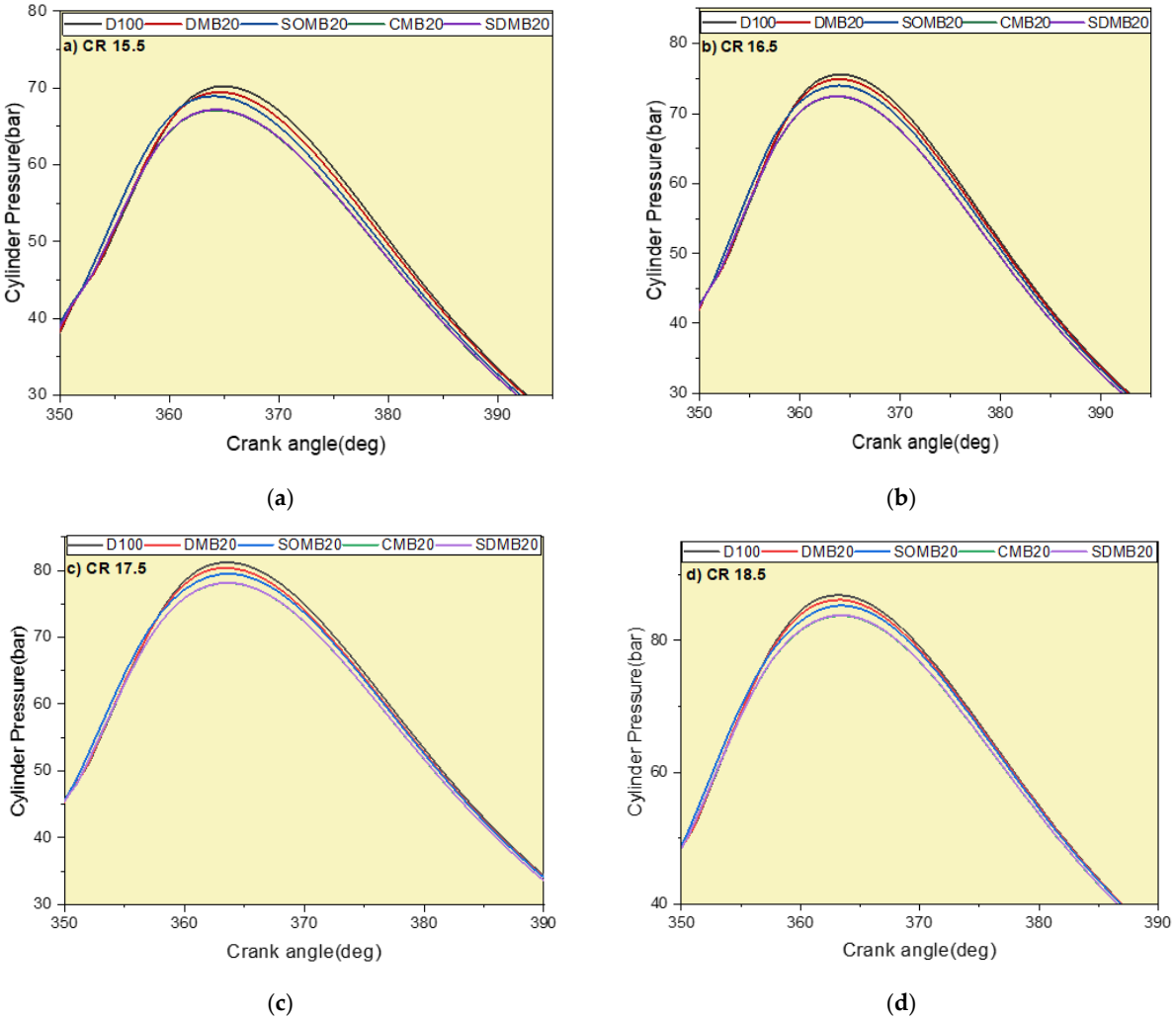

Figure 6. Cylinder pressure wrt crank angle at 100% load at (**a**) CR 15.5, (**b**) CR 16.5, (**c**) CR 17.5, and (**d**) CR 18.5.

3.1.2. Heat Release Rate (HRR)

HRR calculates the conversion of chemical energy into the thermal energy of fuel in the combustion cylinder. The first law of thermodynamics governs the HRR. The HRR is dependent on the pressure peak rise time and cylinder pressure. No heat is released during the process of compression until shortly after fuel injection starts. When gasoline vigorously evaporates and heat is subsequently transmitted to the cylinder walls, the HRR is negative. This comes as a result of total fuel injection and synchronous auto ignition, raising the HRR during the premixed phase. The advancement in injection time, as well as the slow rate of premixed combustion, affect the start of combustion [62,68].

Figure 7 demonstrates that at 100% load conditions, the peak HRR obtained for D100, DMB20, SOMB20, CMB20, and SDMB20 were 34.51 J/deg., 33.70 J/deg., 32.96 J/deg., 30.85 J/deg., and 30.92 J/deg., respectively, for CR 15.5. It can be seen that with an increase in CR (15.5–18.5), the MHRR also increases. The CR has a considerable effect on the HRR during combustion [69]. Additionally, it can be seen from the curves that the initiation of combustion advances as the CR increases. Moreover, biodiesel blends have lower HRR than diesel.

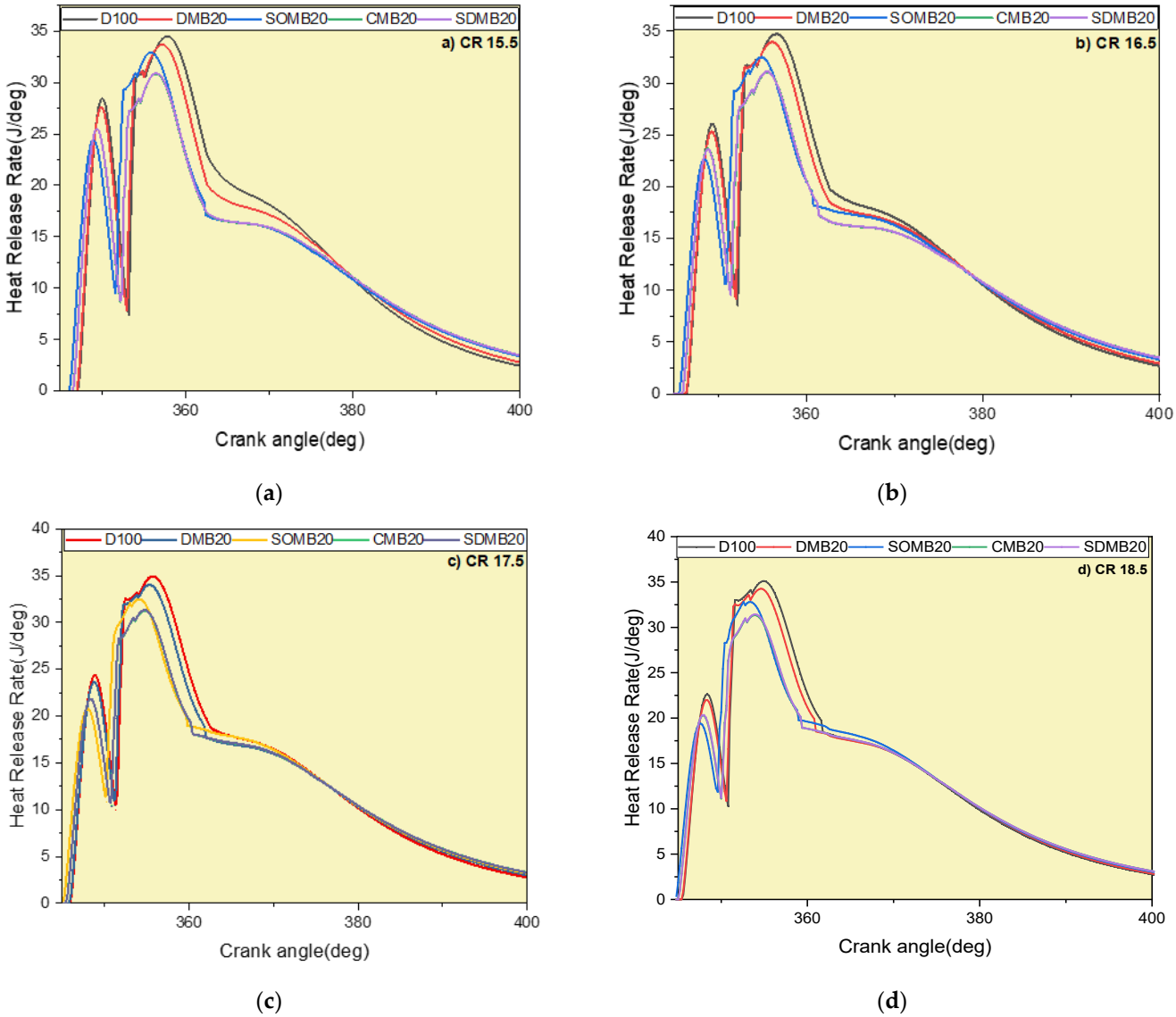

Figure 7. Heat release rate wrt crank angle at (**a**) CR 15.5, (**b**) CR 16.5, (**c**) CR 17.5, and (**d**) CR 18.5.

The HRR graph is often useful for determining the ignition point of combustion [68]. The ignition delays of biodiesel blends were lower than those of diesel, according to HRRs. On the contrary, while running with longer delays, a diesel-powered CI engine was shown to accumulate fuel more quickly, resulting in significantly higher HRRs. Due to shorter ignition delay periods of biodiesel and biodiesel blends when compared to regular diesel, the amount of heat released increases earlier in comparison to regular diesel. As a result, the HRR for biodiesel and its blend were lesser than for diesel fuel because they burned for longer periods of time than diesel fuel and also contained more oxygen [70,71]. The lower heat release rate of biodiesel blends can be validated by previous researchers, such as Bajpai et al. (2009) [72].

3.2. Performance Parameters Analysis

3.2.1. Brake Thermal Efficiency (BTE)

The ratio of an engine's power output to the quantity of energy present in the fuel that was pumped into the combustion chamber is known as the BTE. This crucial property determines how well an engine converts the chemical energy in the fuel into completed work. [73–75]. BTE is lower when compared to diesel fuel due to microalgae biodiesel's lower calorific value and higher viscosity content but rises as engine load increases [76,77].

As observed from Figure 8, at full load condition, the BTE for D100, DMB20, SOMB20, CMB20, and SDMB20 were 34.3%, 33.41%, 33.13%, 32.34%, and 33.38%, respectively, at CR 15.5. Similarly, they were 33.83%, 33.12%, 33.39%, 33.15%, and 33.07%, respectively, at CR 16.5. CR 17.5 results in 33.46%, 32.52%, 32.17%, 32.68%, and 32%, respectively. Additionally, at CR 18.5, the results were 33.06%, 32.26%, 32.03%, 32.35%, and 31.99%, respectively.

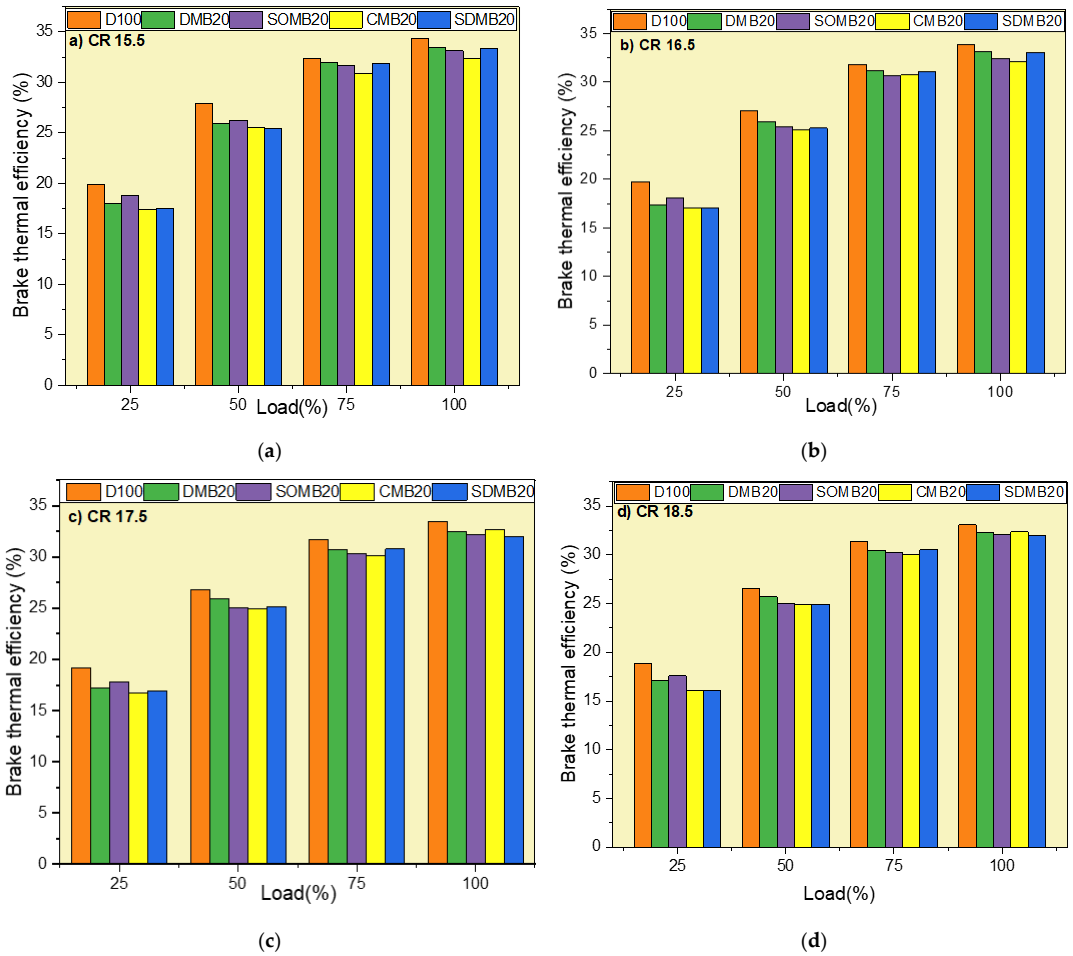

Figure 8. Brake thermal efficiency wrt load at (**a**) CR 15.5, (**b**) CR 16.5, (**c**) CR 17.5, and (**d**) CR 18.5.

For every tested microalgae biodiesel blend, the BTE rises as engine load or braking power rises. This is because a higher cylinder temperature combined with a higher load results in a more efficient combustion process [62,78]. Additionally, BTE decreases with an increase in CR (15.5–17.5) at various loads (%), and BTE is comparatively lower for biodiesel blends than diesel fuel. Almost similar variations for BTE were obtained in the research conducted by N. Krishania et al. (2020) [79].

3.2.2. Exhaust Gas Temperature

The temperature that is reached during the final expansion stroke of the combustion process is EGT. The oxygen concentration of the fuel affects EGT, and as the cetane value of the fuel rises, so does the length of the premixed combustion period. As the fuel will continue to burn continuously until the combustion phase is finished, the quantity of heat emitted will rise [77].

It can be observed in Figure 9, at full load condition, the EGT for D100, DMB20, SOMB20, CMB20, and SDMB20 is 610.96 K, 591.62 K, 599.46 K, 597.88 K, and 597.57 K, respectively, at CR 15.5. Similarly, they are 599.74 K, 587.62 K, 590.92 K, 591.2 K, and 593.04 K, respectively, at CR 16.5. EGT rises when the engine load is increased because more gasoline is pumped into the engine cylinder, increasing heat release. Therefore, the temperature of exhaust gas and that of combustion both rise throughout combustion [80].

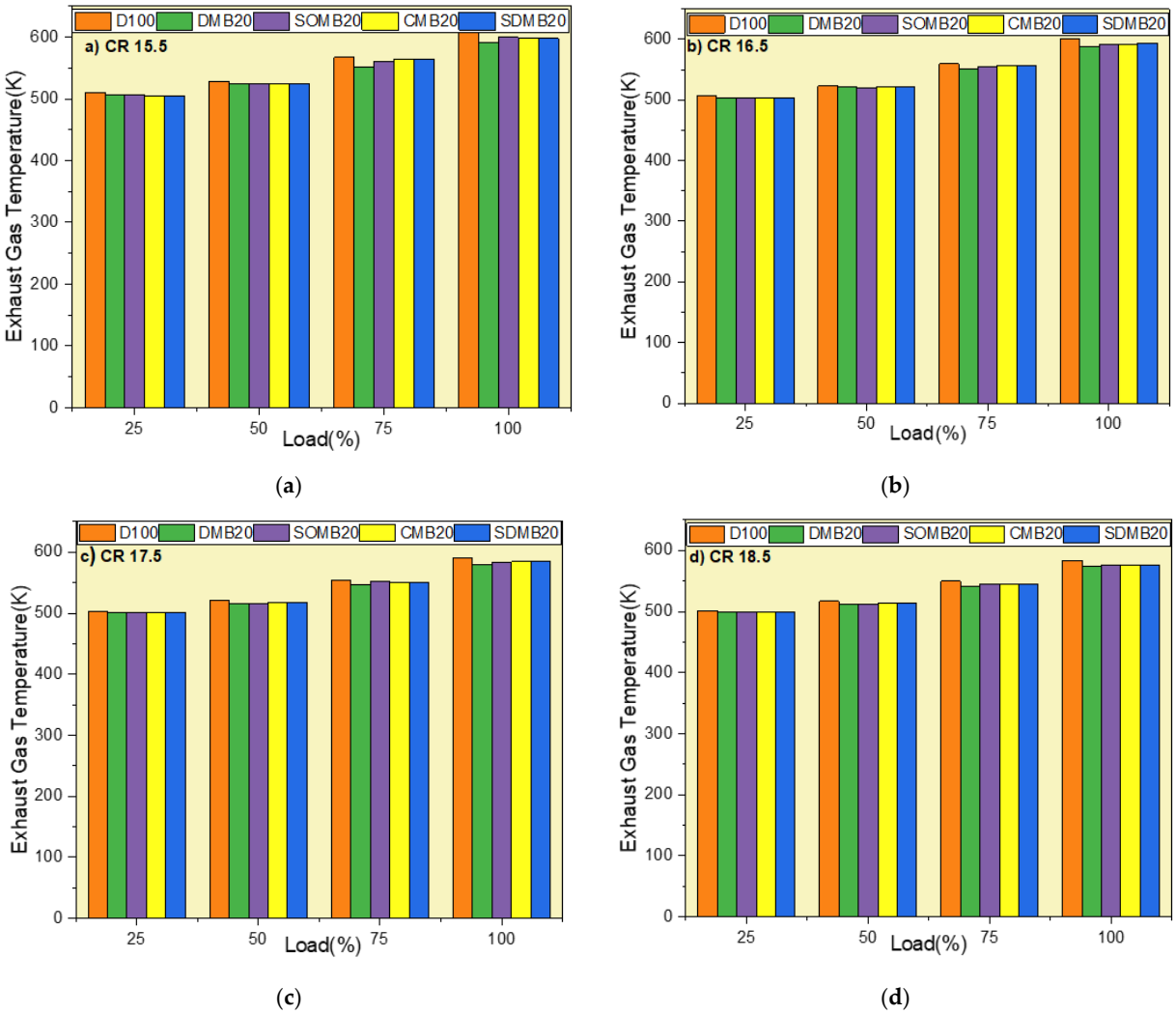

Figure 9. Exhaust gas temperature (K) wrt load (%) at (**a**) CR 15.5, (**b**) CR 16.5, (**c**) CR 17.5, and (**d**) CR 18.5.

According to the graph, as CR increases, EGT reduces for all loads (%) and is lower for all blends in comparison to diesel. Because of the fuel properties, such as more oxygen content, all biodiesel has a lower EGT and thus performs better in the cylinder during combustion [81]. A similar variation in results was seen in the research conducted by U. Rajak et al. (2022), as EGT increases with a rise in CR [58].

3.2.3. Specific Fuel Combustion

The term "Specific fuel consumption" (SFC) refers to the amount of engine power produced per unit quantity of fuel provided by the engine. It is expressed in kilograms per kilowatt-hour (kg/kWh). It was discovered that SFC reduced as engine load increased, pointing to an improvement in the internal combustion engine's combustion efficiency. The density and viscosity of the fuel used in the engine also affect the SFC [82,83].

As observed from Figure 10, at full (100%) load conditions, the SFC for D100, DMB20, SOMB20, CMB20, and SDMB20 is 0.2616 kg/kWh, 0.2644 kg/kWh, 0.2683 kg/kWh, 0.2756 kg/kWh, and 0.2752 kg/kWh, respectively, for CR 15.5. It can be ensured from the figures that with an increase in CR (15.5–18.5), the SFC also increases for all load (%) and diesel and biodiesel blends.

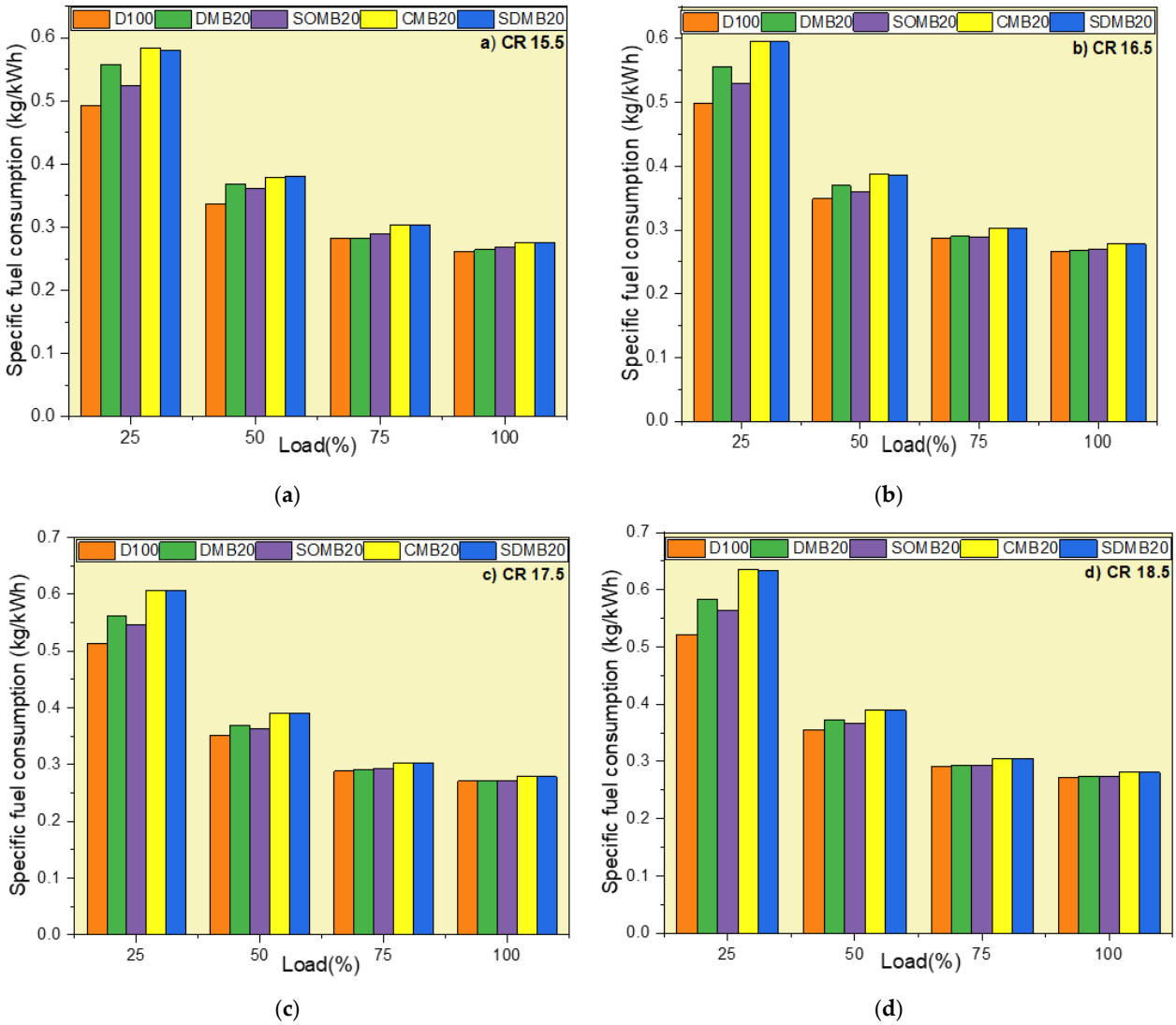

Figure 10. Specific fuel consumption (kg/kWh) wrt load at (**a**) CR 15.5, (**b**) CR 16.5, (**c**) CR 17.5, and (**d**) CR 18.5.

Compared to diesel, the SFC rises with the increase in density and viscosity of biodiesel because more gasoline must be injected into the engine to maintain the same output power [75]. The SFC tends to steady for all biodiesels and their blends as the load increases; however, as the load rises, the SFC drops due to the reduced engine speed [84]. Almost similar variations in results were obtained in the research conducted by N. Krishania et al. (2020) [79].

3.3. Emission Parameters Analysis

3.3.1. NO_X Emission

These emissions are affected by combustion temperature, oxygen content, time taken for combustion reaction, effective combustion zone volume, etc. [85–87]. Figure 11 also shows that all the microalgae biodiesel blends showed an increasing trend in NOx emissions as the engine load increased. More fuel is used as the load rises, which results in more energy being produced during combustion. The increased exhaust gas temperature and longer residence time under higher engine loading conditions were the primary contributors to this growing trend. The results show that a greater biodiesel oxygen content and a blend ratio of biodiesel to diesel lead to increased NOX gas emissions [88,89].

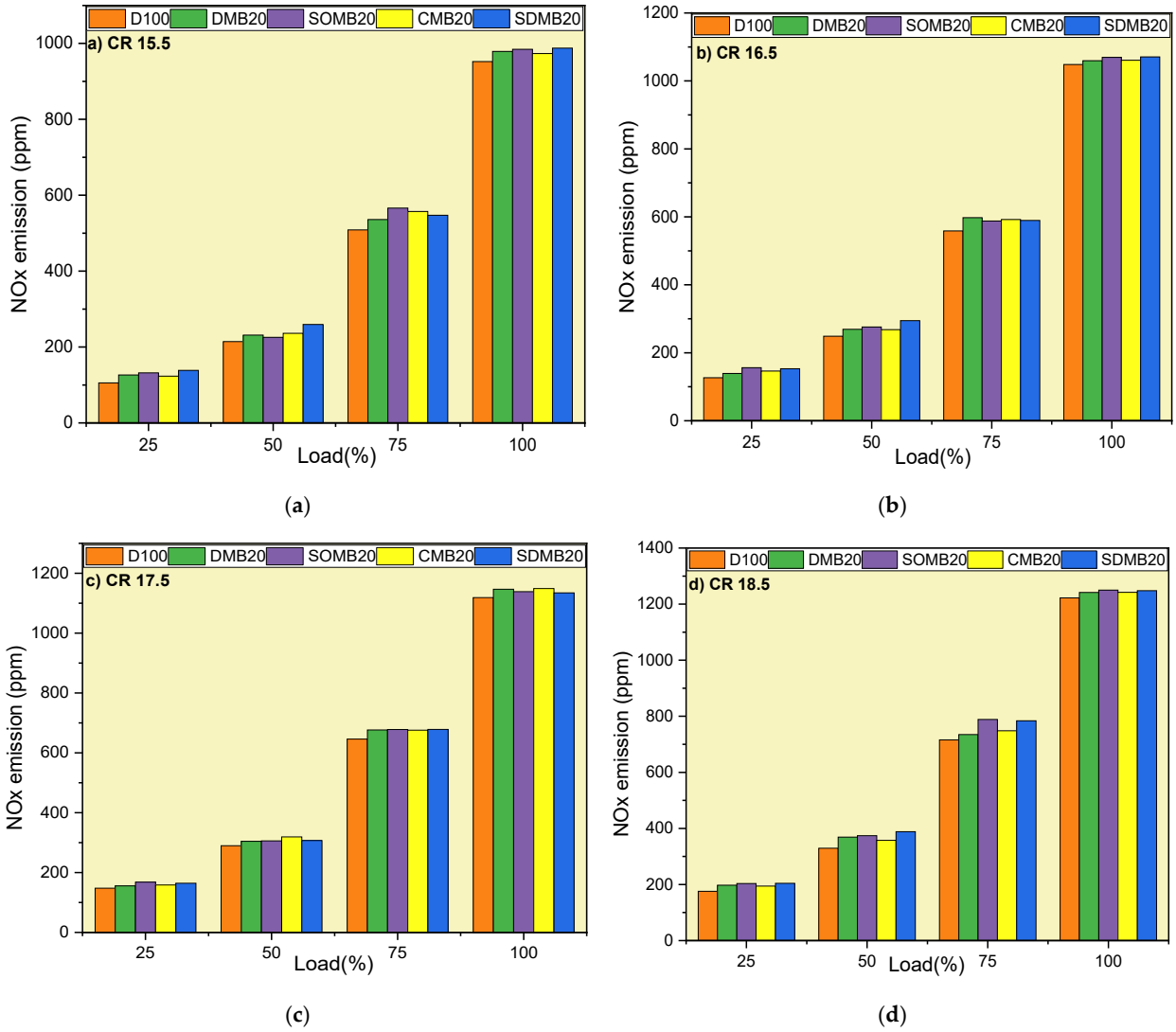

Figure 11. NOx emission(ppm) of different blends wrt load (%) at (**a**) CR 15.5, (**b**) CR 16.5, (**c**) CR 17.5, and (**d**) CR 18.5.

At full load (100%) condition, the NO_x emission for D100, DMB20, SOMB20, CMB20, and SDMB20 were 952.36 ppm, 979.1 ppm, 984.57 ppm, 973.52 ppm, and 987.8 ppm, respectively, at CR 15.5. It can be seen with the rise in CR, the NOx emission increases, and when compared to conventional diesel fuel, NOx emissions for all biodiesel mixes were greater.

Because of homogenous combustion, the rise in CR raised the temperature in the cylinder, increasing NOx emissions. Similar variations in results are shown in U. Rajak et al. (2019) [57] and P. Sharma et al. (2018) [90]. Because of the non-uniform oxidation process, the emission profile increased as the CR increased from 16.5 to 18.5 [91].

3.3.2. CO_2 Emission

CO_2 emissions are directly related to fuel oxygen content. Since all carbon cannot be converted to CO_2, oxygen content that promotes complete combustion explains why using biodiesel blends increases CO_2 emissions [59]. The amount of CO_2 emitted depends on a variety of factors, including viscosity, atomization mechanisms, compression ratio, speed of the engine, and others [80,92].

Figure 12 shows that CO_2 emissions rise in line with an increase in CR and reduce as load increases, and biodiesel blends have comparatively higher CO_2 emissions than diesel fuel. The rate of carbon dioxide emission reduces as the engine load increases, requiring more fuel injection. CO_2 emissions from an engine show the engine's combustion rate [60]. Similar variations in results were obtained by the study done by A. Datta et al. (2016) as CO_2 emission increases with increasing CRs [63].

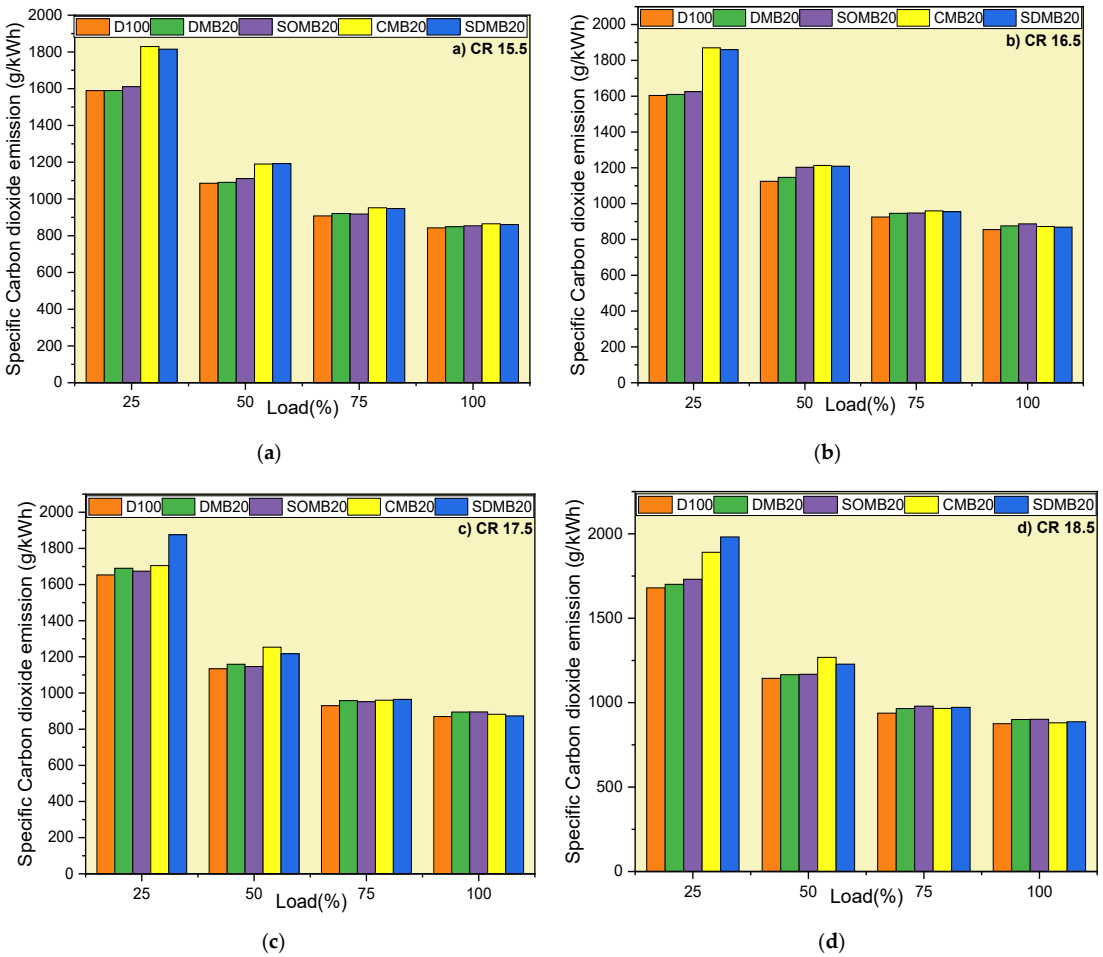

Figure 12. Specific CO_2 emission (ppm) of various microalgae biodiesel blends wrt load (%) at (**a**) CR 15.5, (**b**) CR 16.5, (**c**) CR 17.5, and (**d**) CR 18.5.

3.3.3. PM Emission

PM and carbonaceous particulate formation are the most challenging for diesel engine emissions. Diluted and cooled EGT emits PM emissions. The formation of PM emissions as a result of smoke opacity indicates the presence of dry soot emissions, and PM emissions and smoke emissions are reduced when the engine load increases. The main contributor to the creation of PM emissions is incomplete combustion. PM emissions are influenced by a number of variables, including oxygen concentration, chemical structure, engine load, and latent heat of vaporization. Adding oxygen to the fuel reduces PM emissions during combustion [59,93–97].

Figure 13 shows what happens in conditions of full load: the PM emission for D100, DMB20, SOMB20, CMB20, and SDMB20 were 0.462, 0.436, 0.407, 0.410, and 0.407 g/kWh, respectively, at CR 15.5. Similarly, they were 0.508, 0.463, 0.436, 0.472, and 0.437 g/kWh, respectively, at CR 16.5. Additionally, at CR 17.5, values were 0.527, 0.498, 0.470, 0.502, and 0.471 g/kWh, respectively. Similarly, for CR 18.5 results obtained were 0.539, 0.507, 0.496, 0.514, and 0.494 g/kWh, respectively. It is clear that PM emissions increase as the CR increases, although they decrease for biodiesel blends compared to diesel fuel. According to an earlier study by U. Rajak et al. (2019), increased specific fuel consumption that is associated with higher CRs causes an increase in PM emissions [57]. The specific PME decreased with biodiesel due to higher oxygen content [95,98].

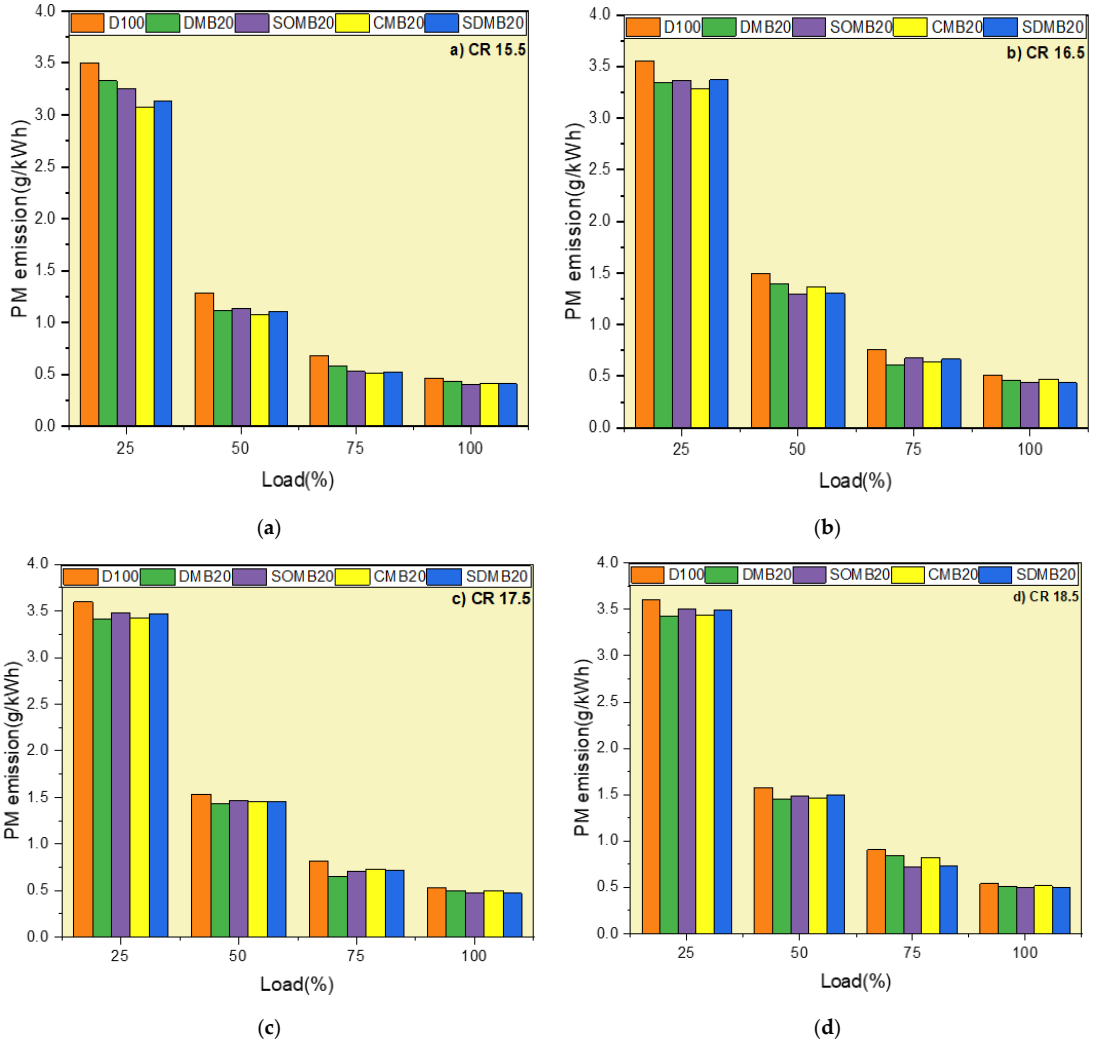

Figure 13. PM (g/kWh) of different microalgae biodiesel blend wrt load (%) at (**a**) CR 15.5, (**b**) CR 16.5, (**c**) CR 17.5, and (**d**) CR 18.5.

3.3.4. Smoke Analysis

In CI engines, smoke emissions are produced by two separate processes: soot formation and oxidation. The rate of soot oxidation is determined by the gas phase collisions, while the rate of soot production is determined by molecular collisions. When the soot oxidation mechanism is activated, smoke emission formation occurs [54,99]. The amount of air in the cylinder affects the amount of smoke that is emitted [100].

As observed from Figure 14, at full load condition, the smoke level for D100, DMB20, SOMB20, CMB20, and SDMB20 were 2.37, 2.22, 2.12, 2.29, and 2.13 BSN, respectively, at CR15.5. Similarly, they were 2.29, 2.192, 2.01, 2.13, and 2.09 BSN, respectively, at CR16.5. Additionally, at CR 17.5, the results obtained were 2.18, 2.04, 1.99, 2.09, and 1.94 BSN, respectively. Similarly, for CR 18.5, values were 2.01, 1.88, 1.82, 1.89, and 1.83 BSN, respectively. From the values, it can be seen that smoke reduces as CR increases. Similar outcomes were attained in the S. Ramalingam et al. (2014) investigation [101].

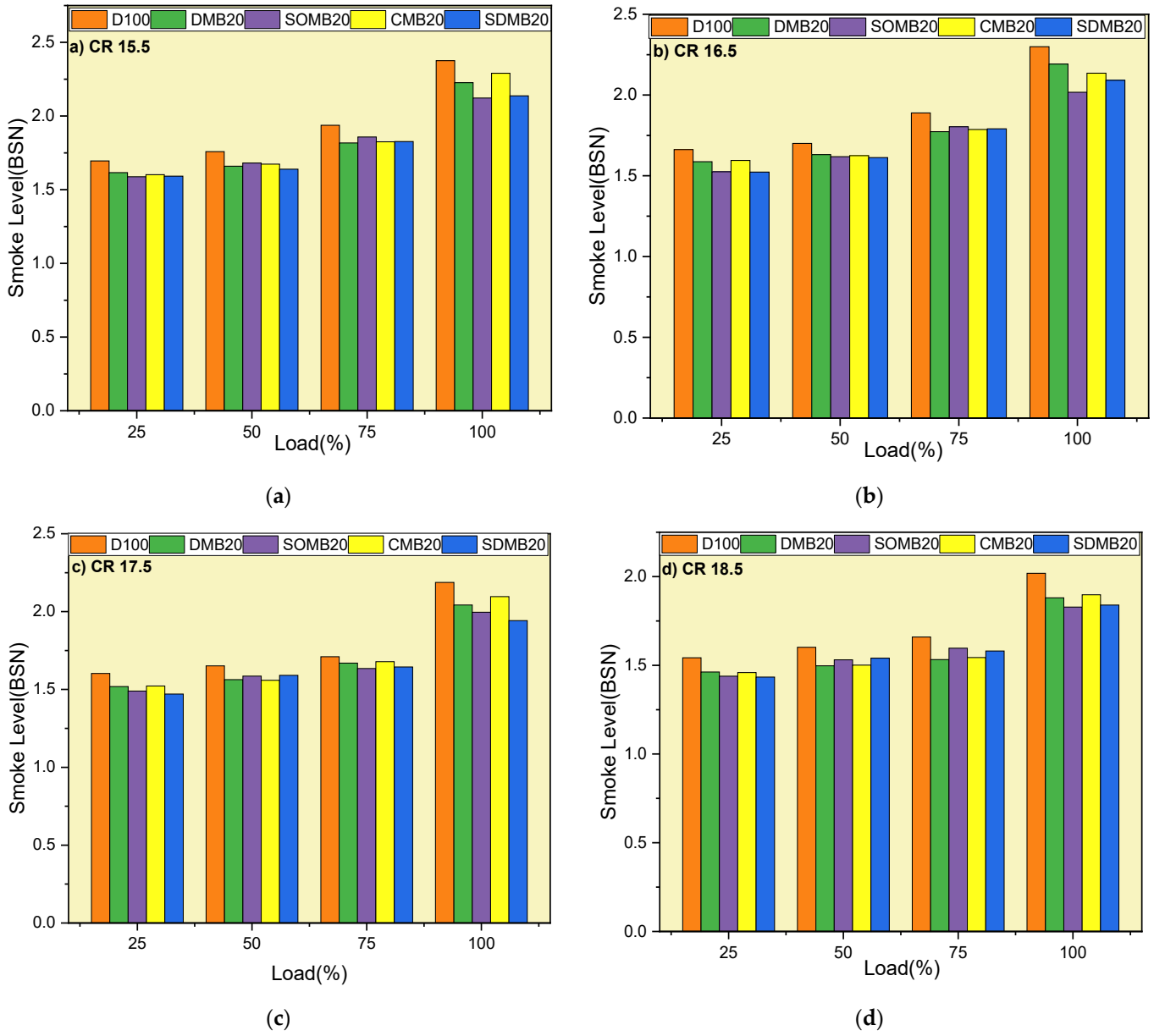

Figure 14. Smoke levels (BSN) of different microalgae biodiesel blends wrt load (%) at (**a**) CR 15.5, (**b**) CR 16.5, (**c**) CR 17.5, (**d**) CR 18.5.

Furthermore, because of the fuel's high oxygen content, diesel's smoke level rises with load whereas biodiesel blends' smoke level falls. Since the oxygen content of diesel is comparatively less accessible, the smoke emission intensity increases with load. Engine load increases smoke emissions because the combustion process is accelerated [98,102].

4. Conclusions

Four different biodiesel blends (DMB20, SOMB20, CMB20, and SDMB20) had their performance, combustion, and emission characteristics investigated and compared to diesel fuel. The numerical study for these biodiesel blends was performed at a stationary natural aspiration, single-cylinder, water-cooled diesel engine with direct injection at a constant engine speed of 1500 rpm and variable CRs (15.5, 16.5, 17.5, and 18.5) with a rated power of 3.7 kW at variable load (25%, 50%, 75%, and 100%).

Among the tested fuel blends, CMB20 had the lowest calorific value, which led to lower thermal efficiency and higher fuel consumption. Similarly, among the tested algae fuel blend, SOMB20 and SDMB20 perform well due to lower density and viscosity. It was found that SOMB20 had the highest cetane number: 51.76.

The primary conclusions of this current investigation are as follows:

- In terms of combustion characteristics, the microalgae biodiesel blends, when compared to petroleum diesel, have less cylinder pressure as biodiesel has a shorter ignition delay. The HRR for biodiesel and its blends were lower than that for diesel because they burn for longer periods of time and contain more oxygen. Irrespective of CRs, minor reductions in CP and HRR were found for DMB20;
- In terms of performance characteristics, SFC for biodiesel blends increased, but BTE and EGT decreased when compared to diesel because the blends that were evaluated had greater heating values and oxygen content. Additionally, with an increase in CRs, SFC increases, while BTE and EGT decrease. The highest increment in SFC was found for CMB20 around 3.27–5.35% with all CRs;
- In terms of emission characteristics, PM and smoke level decrease for all the biodiesel blends, while NOx, as opposed to diesel, and CO_2 rise. As the engine load increases, the rate of CO_2 emission decreases, entailing more fuel injection. With an increase in CRs, the smoke level decreases, while PM, CO_2, and NOx emissions increase. Irrespective of CRs, major reductions in the PM and smoke level were found in SDMB20 and SOMB20 in the range of 8–14%.

It was found from this current study that the biodiesel blend fuel emits higher NOx emissions and has lower BTE and higher SFC consumption compared to fuel. These limitations can be addressed by adding serval other alternative fuels, such as ethanol and hydrogen fuel. Future work should address these challenges, and further experimental work can be conducted to overcome these issues.

Author Contributions: Conceptualization: M.R. and S.K., Methodology, M.R., S.K. and G.D., Formal analyses: M.R. and S.K., Investigation: M.R. and S.K., Data curation: M.R., S.K. and G.D., Writing—original draft: M.R. and S.K., Supervision and project administration and resources: G.D., Review, and editing: S.K. and G.D. All authors have read and agreed to the published version of the manuscript.

Funding: This research received no external funding.

Institutional Review Board Statement: Not Applicable.

Informed Consent Statement: Not Applicable.

Data Availability Statement: All the data is provided within the manuscript.

Conflicts of Interest: The authors declare no conflict of interest.

Nomenclature

BDC	Bottom dead center	BSN	Bosch smoke number
BTE	Brake thermal efficiency	CA	Crank angle
CI	Compression ignition	CR	Compression ratio
CO_2	Carbon dioxide	CP	Cylinder pressure
CMB_{20}	80% diesel + 20% *Chlorella protothecoides* microalgae biodiesel	D100	100% diesel + 0% biodiesel
DMB_{20}	80% diesel + 20% *Dunaliella tertiolecta* microalgae biodiesel	EGT	Exhaust gas temperature
HRR	Heat release rate	PM	Particulate matter
$SOMB_{20}$	SOMB20 80% diesel + 20% *Scenedesmus obliquus* microalgae biodiesel	SDMB20	80% diesel + 20% *Scenedesmus dimorphu* microalgae biodiesel
SFC	Specific fuel consumption	NOx	Oxide of nitrogen

References

1. Abomohra, A.E.-F.; Jin, W.; Tu, R.; Han, S.-F.; Eid, M.; Eladel, H. Microalgal biomass production as a sustainable feedstock for biodiesel: Current status and perspectives. *Renew. Sustain. Energy Rev.* **2016**, *64*, 596–606. [CrossRef]
2. Kalsi, S.S.; Subramanian, K.A. Effect of simulated biogas on performance, combustion and emissions characteristics of a bio-diesel fueled diesel engine. *Renew. Energy* **2017**, *106*, 78–90. [CrossRef]
3. Corrêa, S.M.; Arbilla, G. Carbonyl emissions in diesel and biodiesel exhaust. *Atmos. Environ.* **2008**, *42*, 769–775. [CrossRef]
4. Chang, J.; Leung, D.Y.; Wu, C.; Yuan, Z. A review on the energy production, consumption, and prospect of renewable energy in China. *Renew. Sustain. Energy Rev.* **2003**, *7*, 453–468. [CrossRef]
5. IEA (International Energy Agency). *Key World Energy Statistics 2020*; International Energy Agency India, 2020; Volume 33, p. 4649. Available online: https://www.iea.org/reports/key-world-energy-statistics-2020 (accessed on 17 October 2022).
6. Bharadwaj, S.; Ballare, S.; Rohit; Chandel, M.K. Impact of congestion on greenhouse gas emissions for road transport in Mumbai metropolitan region. *Transp. Res. Procedia* **2017**, *25*, 3538–3551. [CrossRef]
7. IEA (2021). *Tracking Transport*; IEA: Paris, France, 2021; Available online: https://www.iea.org/reports/tracking-transport-2021 (accessed on 17 October 2022).
8. Murugesan, A.; Umarani, C.; Subramanian, R.; Nedunchezhian, N. Bio-diesel as an alternative fuel for diesel engines—A review. *Renew. Sustain. Energy Rev.* **2009**, *13*, 653–662. [CrossRef]
9. Chauhan, S.; Shukla, A. Environmental Impacts of Production of Biodiesel and Its Use in Transportation Sector. *Environ. Impact Biofuels* **2011**, 1–8. [CrossRef]
10. Huang, D.; Zhou, H.; Lin, L. Biodiesel: An Alternative to Conventional Fuel. *Energy Procedia* **2012**, *16*, 1874–1885. [CrossRef]
11. Chandrasekar, K.; Sudhakar, S.; Rajappan, R.; Senthil, S.; Balu, P. Present developments and the reach of alternative fuel: A review. *Mater. Today Proc.* **2021**, *51*, 74–83. [CrossRef]
12. Gumus, M.; Kasifoglu, S. Performance and emission evaluation of a compression ignition engine using a biodiesel (apricot seed kernel oil methyl ester) and its blends with diesel fuel. *Biomass-Bioenergy* **2010**, *34*, 134–139. [CrossRef]
13. Kannan, D.; Pachamuthu, S.; Nabi, N.; Hustad, J.E.; Løvås, T. Theoretical and experimental investigation of diesel engine performance, combustion and emissions analysis fuelled with the blends of ethanol, diesel and jatropha methyl ester. *Energy Convers. Manag.* **2012**, *53*, 322–331. [CrossRef]
14. Fazal, M.; Haseeb, A.; Masjuki, H. Biodiesel feasibility study: An evaluation of material compatibility; performance; emission and engine durability. *Renew. Sustain. Energy Rev.* **2011**, *15*, 1314–1324. [CrossRef]
15. Jaafar, M.N.M.; Safiullah, S. Combustion Characteristics of Rice Bran Oil Biodiesel in an Oil Burner. *J. Teknol.* **2018**, 80. [CrossRef]
16. Bhuiya, M.M.K.; Rasul, M.; Khan, M.; Ashwath, N.; Azad, A.; Hazrat, M. Second generation biodiesel: Potential alternative to-edible oil-derived biodiesel. *Energy Procedia* **2014**, *61*, 1969–1972. [CrossRef]
17. Ahmad, A.L.; Yasin, N.H.M.; Derek, C.J.C.; Lim, J.K. Microalgae as a sustainable energy source for biodiesel production: A review, Renew. *Sustain. Energy Rev.* **2010**, *15*, 584–593. [CrossRef]
18. Suparmaniam, U.; Lam, M.K.; Uemura, Y.; Lim, J.W.; Lee, K.T.; Shuit, S.H. Insights into the microalgae cultivation technology and harvesting process for biofuel production: A review. *Renew. Sustain. Energy Rev.* **2019**, *115*, 109361. [CrossRef]
19. Singh, J.; Gu, S. Commercialization potential of microalgae for biofuels production. *Renew. Sustain. Energy Rev.* **2010**, *14*, 2596–2610. [CrossRef]
20. Amaro, H.M.; Guedes, A.C.; Malcata, F.X. Advances and perspectives in using microalgae to produce biodiesel. *Appl. Energy* **2011**, *88*, 3402–3410. [CrossRef]
21. Khan, S.A.; Rashmi; Hussain, M.Z.; Prasad, S.; Banerjee, U. Prospects of biodiesel production from microalgae in India. *Renew. Sustain. Energy Rev.* **2009**, *13*, 2361–2372. [CrossRef]
22. Aravantinou, A.F.; Theodorakopoulos, M.A.; Manariotis, I.D. Selection of microalgae for wastewater treatment and potential lipids production. *Bioresour. Technol.* **2013**, *147*, 130–134. [CrossRef]

23. Singh, B.; Guldhe, A.; Rawat, I.; Bux, F. Towards a sustainable approach for development of biodiesel from plant and microalgae. *Renew. Sustain. Energy Rev.* **2014**, *29*, 216–245. [CrossRef]
24. Mata, T.M.; Martins, A.A.; Caetano, N.S. Microalgae for biodiesel production and other applications: A review. *Renew. Sustain. Energy Rev.* **2010**, *14*, 217–232. [CrossRef]
25. Islam, M.T.; Rashid, F.; Arefin, A. Numerical analysis of the performance and NOx emission of a diesel engine fueled with algae biofuel-diesel blends. *Energy Sources Part A Recover. Util. Environ. Eff.* **2021**, *43*, 1–20. [CrossRef]
26. Hoekman, S.K.; Robbins, C. Review of the effects of biodiesel on NOx emissions. *Fuel Process. Technol.* **2012**, *96*, 237–249. [CrossRef]
27. Shuping, Z.; Yulong, W.; Mingde, Y.; Kaleem, I.; Chun, L.; Tong, J. Production and characterization of bio-oil from hydrothermal liquefaction of microalgae Dunaliella tertiolecta cake. *Energy* **2010**, *35*, 5406–5411. [CrossRef]
28. Tang, H.; Abunasser, N.; Garcia, M.; Chen, M.E.D.; Ng, K.Y.S.; Salley, S.O. Potential of microalgae oil from Dunaliella tertiolecta as a feedstock for biodiesel. *Appl. Energy* **2011**, *88*, 3324–3330. [CrossRef]
29. da Silva, M.R.O.B.; Moura, Y.A.S.; Converti, A.; Porto, A.L.F.; Marques, D.D.A.V.; Bezerra, R.P. Assessment of the potential of Dunaliella microalgae for different biotechnological applications: A systematic review. *Algal Res.* **2021**, *58*, 102396. [CrossRef]
30. Tizvir, A.; Shojaeefard, M.H.; Zahedi, A.; Molaeimanesh, G.R. Performance and emission characteristics of biodiesel fuel from Dunaliella tertiolecta microalgae. *Renew. Energy* **2021**, *182*, 552–561. [CrossRef]
31. El-Sheekh, M.; Abomohra, A.E.-F.; Eladel, H.; Battah, M.; Mohammed, S. Screening of different species of Scenedesmus isolated from Egyptian freshwater habitats for biodiesel production. *Renew. Energy* **2018**, *129*, 114–120. [CrossRef]
32. El-Baz, F.K.; Gad, M.S.; Abdo, S.M.; Abed, K.A.; Matter, I.A. Performance and Exhaust Emissions of a Diesel Engine Burning Algal Biodiesel Blends. *Fuel* **2016**, *10*, 11.
33. Mandal, S.; Mallick, N. Biodiesel Production by the Green Microalga Scenedesmus obliquus in a Recirculatory Aquaculture System. *Appl. Environ. Microbiol.* **2012**, *78*, 5929–5934. [CrossRef] [PubMed]
34. Chand, G.S.; Richa, G.; Mahavir, Y.; Archana, T. Analysis for the Higher Production of Biodiesel from Scenedesmus dimorphus Algal Species. *Open Access Sci. Rep.* **2012**, *1*, 1–4. [CrossRef]
35. Pugazhendhi, A.; Arvindnarayan, S.; Shobana, S.; Dharmaraja, J.; Vadivel, M.; Atabani, A.E.; Chang, S.W.; Nguyen, D.D.; Kumar, G. Biodiesel from Scenedesmus species: Engine performance, emission characteristics, corrosion inhibition and bioanalysis. *Fuel* **2020**, *276*, 118074. [CrossRef]
36. Al-Lwayzy, S.H.; Yusaf, T. Chlorella protothecoides Microalgae as an Alternative Fuel for Tractor Diesel Engines. *Energies* **2013**, *6*, 766–783. [CrossRef]
37. Patel, A.; Gami, B.; Patel, P.; Patel, B. Biodiesel production from microalgae Dunaliella tertiolecta: A study on economic feasibility on large-scale cultivation systems, Biomass Convers. *Biorefinery* **2021**, *13*, 1071–1085. [CrossRef]
38. Arun, N.; Singh, D.P. Differential response of Dunaliella salina and Dunaliella tertiolecta isolated from brines of Sambhar Salt Lake of Rajasthan (India) to salinities: A study on growth, pigment and glycerol synthesis. *J. Mar. Biol. Assoc. India* **2013**, *55*, 65–70. [CrossRef]
39. Basu, S.; Roy, A.S.; Mohanty, K.; Ghoshal, A.K. Enhanced CO_2 sequestration by a novel microalga: Scenedesmus obliquus SA1 isolated from bio-diversity hotspot region of Assam, India. *Bioresour. Technol.* **2013**, *143*, 369–377. [CrossRef]
40. Chandra, R.; Goswami, D.; Kalita, M.C. Microalgal resources in Chandrapur area, North-East, Assam, India: A perspective for Industrial refinement system and a boon for alternative energy generation and mitigation of green house gases. *Arch. Appl. Sci. Res.* **2012**, *4*, 795–799.
41. Bajwa, K.; Bishnoi, N.R.; Kirrollia, A.; Selvan, S.T. A New Lipid Rich Microalgal SP Scenedesmus Dimorphus Isolated: Nile Red Staining and Effect of Carbon, Nitrogen Sources on its Physio-Biochemical Components. *Eur. J. Sustain. Dev. Res.* **2018**, *2*, 43. [CrossRef]
42. Arvindnarayan, S.; Shobana, S.; Dharmaraja, J.; Nguyen, D.D.; Chang, S.W.; Atabani, A.E.; Kumar, G.; Prabhu, K.K.S. Spectral, In Vitro Biological, Engine and Emission Performances of Biodiesel Production from Chlorella protothecoides: A Sustainable Renewable Energy Source. *Waste Biomass-Valorization* **2020**, *11*, 5809–5819. [CrossRef]
43. Piloto-Rodríguez, R.; Sánchez-Borroto, Y.; Melo-Espinosa, E.A.; Verhelst, S. Assessment of diesel engine performance when fueled with biodiesel from algae and microalgae: An overview. *Renew. Sustain. Energy Rev.* **2017**, *69*, 833–842. [CrossRef]
44. Tang, D.; Han, W.; Li, P.; Miao, X.; Zhong, J. CO_2 biofixation and fatty acid composition of Scenedesmus obliquus and Chlorella pyrenoidosa in response to different CO_2 levels. *Bioresour. Technol.* **2011**, *102*, 3071–3076. [CrossRef] [PubMed]
45. Tsaousis, P.; Wang, Y.; Roskilly, A.P.; Caldwell, G.S. Algae to Energy: Engine Performance Using Raw Algal Oil. *Energy Procedia* **2014**, *61*, 656–659. [CrossRef]
46. British Standard Institution. Automotive Fuels—Fatty Acid Methyl Esters (FAME) for Diesel Engines—Requirements and Test Methods; Br. Stand. Inst., European Union 2010; p. 22. Available online: http://agrifuelsqcs-i.com/attachments/1598/en14214.pdf (accessed on 19 October 2022).
47. *IS 15607*; Bio-Diesel (B 100) Blend Stock for Diesel Fuel. Bureau of Indian Standards: Bhopal, India, 2005.
48. Yaşar, F.; Altun, Ş. Biodiesel properties of microalgae (*Chlorella protothecoides*) oil for use in diesel engines. *Int. J. Green Energy* **2018**, *15*, 941–946. [CrossRef]
49. Subramaniam, M.; Solomon, J.M.; Nadanakumar, V.; Anaimuthu, S.; Sathyamurthy, R. Experimental investigation on performance, combustion and emission characteristics of DI diesel engine using algae as a biodiesel. *Energy Rep.* **2020**, *6*, 1382–1392. [CrossRef]

50. Rajak, U.; Nashine, P.; Verma, T.N. Effect of fuel injection pressure of microalgae spirulina biodiesel blends on engine characteristics. *J. Comput. Appl. Res. Mech. Eng.* **2021**, *10*, 113–125. [CrossRef]
51. Datta, A.; Mandal, B.K. Engine performance, combustion and emission characteristics of a compression ignition engine operating on different biodiesel-alcohol blends. *Energy* **2017**, *125*, 470–483. [CrossRef]
52. Prabu, S.S.; Asokan, M.A.; Roy, R.; Francis, S.; Sreelekh, M.K. Performance, combustion and emission characteristics of diesel engine fuelled with waste cooking oil bio-diesel/diesel blends with additives. *Energy* **2017**, *122*, 638–648. [CrossRef]
53. Sachuthananthan, B.; Krupakaran, R.L.; Balaji, G. Exploration on the behaviour pattern of a DI diesel engine using magnesium oxide nano additive with plastic pyrolysis oil as alternate fuel. *Int. J. Ambient. Energy* **2021**, *42*, 701–712. [CrossRef]
54. Rajak, U.; Nashine, P.; Verma, T.N. Assessment of diesel engine performance using spirulina microalgae biodiesel. *Energy* **2019**, *166*, 1025–1036. [CrossRef]
55. Yadav, B.; Noguchi, R.; Soni, P.; Abah, E.; Yadav, C.B. Performance evaluation and emission characteristics of microalgae fuel in combustion engine. *J. Pharmacogn. Phytochem.* **2018**, *7*, 2319–2326.
56. Fiveland, S.B.; Assanis, D.N. A Four-Stroke Homogeneous Charge Compression Ignition Engine Simulation for Combustion and Performance Studies. *J. Engines* **2000**, *109*, 452–468. [CrossRef]
57. Rajak, U.; Nashine, P.; Verma, T.N.; Pugazhendhi, A. Performance, combustion and emission analysis of microalgae Spirulina in a common rail direct injection diesel engine. *Fuel* **2019**, *255*, 115855. [CrossRef]
58. Rajak, U.; Nashine, P.; Dasore, A.; Verma, T.N. Utilization of renewable and sustainable microalgae biodiesel for reducing the engine emissions in a diesel engine. *Fuel* **2022**, *311*, 122498. [CrossRef]
59. Rajak, U.; Nashine, P.; Verma, T.N. Verma, Comparative Assessment of The Emission Characteristics of First, Second and Third Generation Biodiesels As Fuel in A Diesel Engine. *J. Therm. Eng.* **2020**, *6*, 211–225. [CrossRef]
60. Kesharvani, S.; Dwivedi, G.; Verma, T.N.; Verma, P. The Experimental Investigation of a Diesel Engine Using Ternary Blends of Algae Biodiesel, Ethanol and Diesel Fuels. *Energies* **2023**, *16*, 229. [CrossRef]
61. Rajak, U.; Nashine, P.; Verma, T.N. Verma, Characteristics of microalgae spirulina biodiesel with the impact of n-butanol addition on a CI engine. *Energy* **2019**, *189*, 116311. [CrossRef]
62. Al-Dawody, M.F.; Bhatti, S.K. Optimization strategies to reduce the biodiesel NOx effect in diesel engine with experimental verification. *Energy Convers. Manag.* **2013**, *68*, 96–104. [CrossRef]
63. Datta, A.; Mandal, B.K. Effect of compression ratio on the performance, combustion and emission from a diesel engine using palm biodiesel. *AIP Conf. Proc.* **2016**, *1754*, 050005. [CrossRef]
64. Shrivastava, P.; Verma, T.N. An experimental investigation into engine characteristics fueled with Lal ambari biodiesel and its blends. *Therm. Sci. Eng. Prog.* **2020**, *17*, 100356. [CrossRef]
65. Wei, L.; Cheung, C.; Ning, Z. Influence of waste cooking oil biodiesel on combustion, unregulated gaseous emissions and particulate emissions of a direct-injection diesel engine. *Energy* **2017**, *127*, 175–185. [CrossRef]
66. Gnanasekaran, S.; Saravanan, N.; Ilangkumaran, M. Influence of injection timing on performance, emission and combustion characteristics of a DI diesel engine running on fish oil biodiesel. *Energy* **2016**, *116*, 1218–1229. [CrossRef]
67. Bora, B.J.; Saha, U.K.; Chatterjee, S.; Veer, V. Veer, Effect of compression ratio on performance, combustion and emission characteristics of a dual fuel diesel engine run on raw biogas. *Energy Convers. Manag.* **2014**, *87*, 1000–1009. [CrossRef]
68. Jamuwa, D.K.; Sharma, D.; Soni, S.L. Experimental investigation of performance, exhaust emission and combustion parameters of stationary compression ignition engine using ethanol fumigation in dual fuel mode. *Energy Convers. Manag.* **2016**, *115*, 221–231. [CrossRef]
69. Forero, J.D.; Valencia, G.E.; Obregon, L.G. Study of the influence of compression ratio on the rate of heat release in small displacement Diesel engines. *Indian J. Sci. Technol.* **2018**, *11*, 1–8. [CrossRef]
70. Kalam, M.A.; Masjuki, H.H. Emissions and deposit characteristics of a small diesel engine when operated on preheated crude palm oil. *Biomass Bioenergy* **2004**, *27*, 289–297. [CrossRef]
71. Sanjid, A.; Masjuki, H.H.; Kalam, M.A.; Rahman, S.M.A.; Abedin, M.J.; Palash, S.M. Production of palm and jatropha based biodiesel and investigation of palm-jatropha combined blend properties, performance, exhaust emission and noise in an unmodified diesel engine. *J. Clean. Prod.* **2014**, *65*, 295–303. [CrossRef]
72. Bajpai, S.; Sahoo, P.K.; Das, L.M. Feasibility of blending karanja vegetable oil in petro-diesel and utilization in a direct injection diesel engine. *Fuel* **2009**, *88*, 705–711. [CrossRef]
73. Pereira, R.G.; Tulcan, O.E.P.; Fellows, C.E.; De Jesus Lameira, V.; Quelhas, O.L.G.; Elias De Aguiar, M.; Filho, D.M.D.E.S. Sustainability and mitigation of greenhouse gases using ethyl beef tallow biodiesel in energy generation. *J. Clean. Prod.* **2012**, *29–30*, 269–276. [CrossRef]
74. Fattah, I.M.R.; Hassan, M.H.; Kalam, M.A.; Atabani, A.E.; Abedin, M.J. Synthetic phenolic antioxidants to biodiesel: Path toward NOx reduction of an unmodified indirect injection diesel engine. *J. Clean. Prod.* **2014**, *79*, 82–90. [CrossRef]
75. Sakthivel, R.; Ramesh, K.; Purnachandran, R.; Shameer, P.M. A review on the properties, performance and emission aspects of the third-generation biodiesels. *Renew. Sustain. Energy Rev.* **2018**, *82*, 2970–2992. [CrossRef]
76. Gogoi, T.K.; Baruah, D.C. The use of Koroch seed oil methyl ester blends as fuel in a diesel engine. *Appl. Energy* **2011**, *88*, 2713–2725. [CrossRef]

77. Dhamodaran, G.; Krishnan, R.; Pochareddy, Y.K.; Pyarelal, H.M.; Sivasubramanian, H.; Ganeshram, A.K. A comparative study of combustion, emission, and performance characteristics of rice-bran-, neem-, and cottonseed-oil biodiesels with varying degree of unsaturation. *Fuel* **2017**, *187*, 296–305. [CrossRef]
78. Syed, A.; Quadri, S.A.P.; Rao, G.A.P.; Mohd, W. Experimental investigations on DI (direct injection) diesel engine operated on dual fuel mode with hydrogen and mahua oil methyl ester (MOME) as injected fuels and effects of injection opening pressure. *Appl. Therm. Eng.* **2017**, *114*, 118–129. [CrossRef]
79. Krishania, N.; Rajak, U.; Chaurasiya, P.; Singh, T.; Birru, A.; Verma, T. Investigations of spirulina, waste cooking and animal fats blended biodiesel fuel on auto-ignition diesel engine performance, emission characteristics. *Fuel* **2020**, *276*, 118123. [CrossRef]
80. Gharehghani, A.; Mirsalim, M.; Hosseini, R. Effects of waste fish oil biodiesel on diesel engine combustion characteristics and emission. *Renew. Energy* **2017**, *101*, 930–936. [CrossRef]
81. Jiao, Y.; Liu, R.; Zhang, Z.; Yang, C.; Zhou, G.; Dong, S.; Liu, W. Comparison of combustion and emission characteristics of a diesel engine fueled with diesel and methanol-Fischer-Tropsch diesel-biodiesel-diesel blends at various altitudes. *Fuel* **2019**, *243*, 52–59. [CrossRef]
82. Datta, A.; Mandal, B.K. Impact of alcohol addition to diesel on the performance combustion and emissions of a compression ignition engine. *Appl. Therm. Eng.* **2016**, *98*, 670–682. [CrossRef]
83. Sathiyamoorthi, R.; Sankaranarayanan, G. The effects of using ethanol as additive on the combustion and emissions of a direct injection diesel engine fuelled with neat lemongrass oil-diesel fuel blend. *Renew. Energy* **2017**, *101*, 747–756. [CrossRef]
84. Rajak, U.; Nashine, P.; Singh, T.S.; Verma, T.N. Numerical investigation of performance, combustion and emission characteristics of various biofuels. *Energy Convers. Manag.* **2018**, *156*, 235–252. [CrossRef]
85. Şahin, Z.; Aksu, O.N. Experimental investigation of the effects of using low ratio n-butanol/diesel fuel blends on engine performance and exhaust emissions in a turbocharged DI diesel engine. *Renew. Energy* **2015**, *77*, 279–290. [CrossRef]
86. Wu, H.W.; Wu, Z.Y. Investigation on combustion characteristics and emissions of diesel/hydrogen mixtures by using energy-share method in a diesel engine. *Appl. Therm. Eng.* **2012**, *42*, 154–162. [CrossRef]
87. Wamankar, A.K.; Satapathy, A.K.; Murugan, S. Experimental investigation of the effect of compression ratio, injection timing & pressure in a DI (direct injection) diesel engine running on carbon black-water-diesel emulsion. *Energy* **2015**, *93*, 511–520. [CrossRef]
88. Kuleshov, A.; Mahkamov, K. Multi-zone diesel fuel spray combustion model for the simulation of a diesel engine running on biofuel. *Proc. Inst. Mech. Eng. Part A J. Power Energy* **2008**, *222*, 309–321. [CrossRef]
89. Rajak, U.; Verma, T.N. Effect of emission from ethylic biodiesel of edible and non-edible vegetable oil, animal fats, waste oil and alcohol in CI engine. *Energy Convers. Manag.* **2018**, *166*, 704–718. [CrossRef]
90. Sharma, P.; Dhar, A. Compression ratio influence on combustion and emissions characteristic of hydrogen diesel dual fuel CI engine: Numerical Study. *Fuel* **2018**, *222*, 852–858. [CrossRef]
91. Senthil, M.; Visagavel, K.; Saravanan, C.G.; Rajendran, K. Rajendran, Investigations of red mud as a catalyst in Mahua oil biodiesel production and its engine performance. *Fuel Process Technol.* **2016**, *149*, 7–14. [CrossRef]
92. Rahman, S.M.A.; Masjuki, H.H.; Kalam, M.A.; Abedin, M.J.; Sanjid, A.; Sajjad, H. Production of palm and *Calophyllum inophyllum* based biodiesel and investigation of blend performance and exhaust emission in an unmodified diesel engine at high idling conditions. *Energy Convers. Manag.* **2013**, *76*, 362–367. [CrossRef]
93. Singh, T.S.; Rajak, U.; Verma, T.N.; Nashine, P.; Mehboob, H.; Manokar, A.M.; Afzal, A. Exhaust emission characteristics study of light and heavy-duty diesel vehicles in India. *Case Stud. Therm. Eng.* **2021**, *29*, 101709. [CrossRef]
94. Kesharvani, S.; Verma, T.N.; Dwivedi, G. Computational analysis of chlorella protothecoides biofuels on engine combustion, performance and emission. *Sustain. Energy Technol. Assess.* **2023**, *55*, 102972. [CrossRef]
95. Rajak, U.; Verma, T.N. Influence of combustion and emission characteristics on a compression ignition engine from a different generation of biodiesel. *Eng. Sci. Technol. Int. J.* **2020**, *23*, 10–20. [CrossRef]
96. Rajak, U.; Nashine, P.; Verma, T.N. Performance analysis and exhaust emissions of aegle methyl ester operated compression ignition engine. *Therm. Sci. Eng. Prog.* **2019**, *12*, 100354. [CrossRef]
97. Shrivastava, P.; Verma, T.N.; Pugazhendhi, A. An experimental evaluation of engine performance and emisssion characteristics of CI engine operated with Roselle and Karanja biodiesel. *Fuel* **2019**, *254*, 115652. [CrossRef]
98. Rajak, U.; Verma, T.N. A comparative analysis of engine characteristics from various biodiesels: Numerical study. *Energy Convers. Manag.* **2019**, *180*, 904–923. [CrossRef]
99. Emiroğlu, A.O.; Şen, M. Combustion, performance and exhaust emission characterizations of a diesel engine operating with a ternary blend (alcohol-biodiesel-diesel fuel). *Appl. Therm. Eng.* **2018**, *133*, 371–380. [CrossRef]
100. Karthickeyan, V.; Thiyagarajan, S.; Ashok, B.; Geo, V.E.; Azad, A. Experimental investigation of pomegranate oil methyl ester in ceramic coated engine at different operating condition in direct injection diesel engine with energy and exergy analysis. *Energy Convers. Manag.* **2020**, *205*, 112334. [CrossRef]

101. Ramalingam, S.; Chinnaia, P.; Rajendran, S. Influence of Compression Ratio on the Performance and Emission Characteristics of Annona Methyl Ester Operated di Diesel Engine. *Adv. Mech. Eng.* **2014**, *6*, 17–19. [CrossRef]
102. Liu, J.; Sun, P.; Huang, H.; Meng, J.; Yao, X. Experimental investigation on performance, combustion and emission characteristics of a common-rail diesel engine fueled with polyoxymethylene dimethyl ethers-diesel blends. *Appl. Energy* **2017**, *202*, 527–536. [CrossRef]